Cassini RTG Program CDRL Transmittal

TO:
U.S. Department of Energy
6633 Canoga Avenue
Canoga Park, California 91303
Attention: K. Vijaiyan
Project Manager

DISTRIBUTION:

Symbol	Copies
A	5
B	1
C	1
D	1
E	2
H	2
J	20
K	1

Cassini RTG Program
Contract No: DE-AC03-91SF18852

In Reply Refer to: **CON #1357**
Date: **24 October 1995**

CDRL Number: **Reporting Requirement 4.F (Document No. RR16)**

Title: **Semi Annual Technical Progress Report (3 April 1995 through 1 October 1995)**

Approval Requirements:

Approval [ ] None [X]

Contract Period: **11 January 1991 through 30 April 1998**

INTRODUCTION

The technical progress achieved during the period 3 April 1995 through 1 October 1995 on Contract DE-AC03-91SF18852 Radioisotope Thermoelectric Generators and Ancillary Activities is described herein. Monthly technical activity for the period 28 August 1995 through 1 October 1995 is included in this Semi Annual Technical Progress Report.

This report is organized by program task structure.

- 1.X Spacecraft Integration and Liaison
- 2.X Engineering Support
- 3.X Safety
- 4.X Qualified Unicouple Production
- 5.X ETG Fabrication, Assembly, and Test
- 6.X Ground Support Equipment (GSE)
- 7.X RTG Shipping and Launch Support
- 8.X Designs, Reviews, and Mission Applications
- 9.X Project Management, Quality Assurance, Reliability, Contract Changes, CAGO Acquisition (Operating Funds), and CAGO Maintenance and Repair
- H.X CAGO Acquisition (Capital Funds)

Note: Task H.X scope is included in SOW ¶ Task 9.5.
Task H. was created to manage CAGO acquired with capital equipment funding.

Approved: R. J. Hemler, Manager
Space Power Programs

Internal Distribution:
Technical Report List

From: Lockheed Martin Astro Space
Room 10B50 Building B
720 Vandenberg Road
King of Prussia, PA 19406

Signature:
Joseph M. Waks
Contracts Manager

LOCKHEED MARTIN

LOCKHEED MARTIN ASTRO SPACE

Contract No.
DE-AC03-91SF18852

GPHS - RTGs

In Support of the

Cassini RTG Program

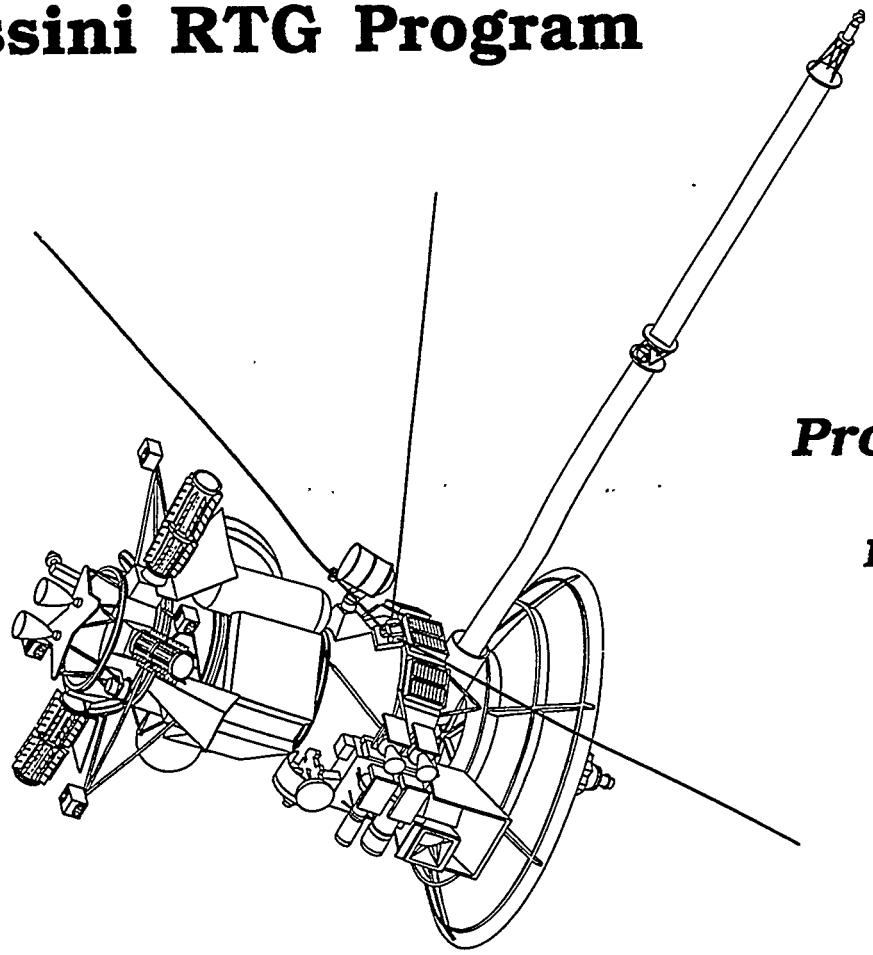

Semi Annual Technical Progress Report

Document No. RR16

3 April 1995
through
1 October 1995

20 October 1995

Space Power Programs

HH

Semi Annual Technical Report

Contract No.
DE-AC03-91SF18852

GPHS-RTGs in Support of the Cassini Mission

Document No. RR16

3 April 1995
through
1 October 1995

Prepared for:

U.S. Department of Energy
Oakland Operations Office
1301 Clay Street
Oakland, CA 94612-5208

Prepared by:

Lockheed Martin Astro Space
P.O. Box 8555
Philadelphia, PA 19101

LOCKHEED MARTIN

Space Power Programs

Semi Annual Technical Progress Report

The technical progress achieved during the period 3 April 1995 through 1 October 1995 on Contract No. DE-AC03-91SF18852, Radioisotope Generators and Ancillary Activities is described herein.

This report is organized by the program task structure as follows:

Table of Contents

List of Illustrations

List of Illustrations (Cont'd)

List of Tables

Task 1

Spacecraft Integration and Liaison

TASK 1
SPACECRAFT INTEGRATION AND LIAISON

Based on the F-5 low level testing at Mound and the full size spacecraft acoustic testing at Denver, agreement was reached with JPL on the random acceptance test levels for the Cassini mission. The new test levels were incorporated by JPL into an updated draft of the Cassini Orbiter Environments and Testing Specification (ES 515803). Further, JPL added definition of the spacecraft propulsion nozzle plume thermal environment. With these matters finalized the specification was forwarded to DOE for final review and sign-off.

Also during this reporting period, informal discussions were held at JPL to review progress on the preparation of the designs for the new RTG installation cart and related fixturing. The equipment (operating through openings in the payload fairing) will be used to install the RTGs on the spacecraft. The meetings concluded that work on the designs was progressing satisfactorily.

Preliminary information was prepared to predict the effects of greater than normal helium build-up on RTG electrical power output. Such helium build-up could occur if the launch was delayed after the RTGs were installed on the spacecraft. Preliminary information for a 90-day build-up period was forwarded to JPL. At the end of this report period, studies were in progress to evaluate the effects of other build-up periods.

Agreement was reached on the approach to be followed for obtaining specific test data requested by JPL. The additional data involves 1) measurements to better define the ambient magnetic field during RTG magnetic field testing, 2) measurement of the RTG inboard end dome temperature, and 3) measurement of the generator thermopile-to-case capacitance. The request concerning the ambient magnetic field measurements was incorporated into the magnetic testing of the F-5 RTG accomplished at Mound during this reporting period. The request for the measurement of the end dome temperature was to have been completed during the thermal vacuum (T/V) testing of the F-5 RTG. However, difficulty with the temperature sensing probe in contact with the end dome, prevented accurate measurement of the requested temperature. Another opportunity for measuring the temperature of the flight dome under vacuum conditions will occur with the T/V testing of the F-2 RTG. However, this test is not scheduled until next spring. JPL has the matter under consideration. The measurement concerning the thermopile-to-case capacitance is planned to be accomplished on the E-7 ETG at Lockheed Martin Astro Space during vacuum processing early next year.

Task 2

Engineering Support

TASK 2
ENGINEERING SUPPORT

Specifications/Drawings

Throughout this period ECNs for the ETG/RTG and unicouple activities were prepared and processed through CCB approval.

During this period the environmental requirements were finalized with JPL and, as a result, the following specifications were completed and issued:

- Product Specification for the General Purpose Heat Source (PS23009146)
- Product Specification for the General Purpose Heat Source - ETG (PS23009147)

The following specifications were prepared and submitted to DOE for approval:

- Environmental Criteria and Test Requirements for the GPHS-RTG (PS23009150)
- Product Specification for the GPHS-RTG (PS23009148)
- System Specification for the GPHS-RTG (SS23009149)

Also issued in August was the RTG Design Qualification Report (Milestone #10) as CDRL B.16.

Qualification RTD Harness and Cable Assembly

The Qualification Report for the Cassini RTD and Cable Assembly was issued on 7 August 1995 (Ref. PIR-1VC2-Cassini-099). The final report of the FRB on the Qualification RTD Cable Assembly was issued on 14 August 1995 as a Topical Report (CDRL B.3). The submittal of these two reports completed the qualification RTD harness and cable assembly activities.

RTG Fuel Form, Fueling, and Test Support/Liaison

Support of heat source fabrication activities at the DOE National Laboratories continued with the review and disposition of production related non-conformances. In addition, specification and procedure revisions were also reviewed. A review was held at Los Alamos to discuss ultrasonic and radiographic examination of the capsule girth seal weld.

The F-2 heat source module stack-up was reviewed. Based on module measurement data provided by Mound, it was concluded that the stack parallelism requirements would be met for the three units to be fueled. Further, it was concluded that the stacking order for the F-2 heat source would provide an acceptable axial heat distribution. Decisions on the acceptability of the stacking order for the other two heat sources to be fueled must await the fabrication and delivery of the required fueled clads to Mound.

Task 3

Safety

TASK 3
SAFETY ANALYSIS TASK

Safety Analysis Task

The safety analysis task is comprised of four major activities: 1) Launch Accident Analysis; 2) Reentry Analysis; 3) Consequence and Risk Analysis and 4) the Safety Test Program. An overview of the significant issues related to this task for this six month period, followed by details in each of the four major activities, is provided in the following subsections.

For the launch accident analysis a substantial amount of support was directed towards finalizing the Databook accident and environment inputs. At the initial portion of this reporting period the lack of concrete definition adversely impacted the effort to develop the LASEP-T analysis software. Through a series of reviews with JPL, Lockheed Martin SLS-Denver, NASA LeRC, and DOE, concerns related to the draft accident and environment documentation issued in March through April 1995 were resolved, and a workable version of the accident and environment definition was finally generated late June 1995. With the incorporation of minor updates to this definition a formal issue of the Databook (Rev. 0) was finally received mid-September 1995. Consistent with the availability of well defined accident/environment data, significant progress on the LASEP-T code was achieved in the July 1995 - September 1995 reporting period. A discussion of this progress is provided in the following launch accident analysis subsection.

The Databook issued in September 1995 contained a listing of open items which must be resolved. With regard to the launch accident analysis work, the two major open issues are: 1) Definition of SRMU Propellant Fallback Environment; and 2) Resolution of the accident case termed "Flight Hardware/RTG Impact." To prevent further disruption on the LASEP-T development schedule these items have been segregated from current activities and are tentatively planned to be addressed by an addendum to the FSAR.

There are also minor accident/environment issues which must be resolved before performing the LASEP-T runs (planned for November 1995 start), however, these are not currently delaying the development work. A review of the Rev. 0 Databook, which

is presently being conducted, will examine the previous list of open issues (Ref: CON #1208 dated 3 May 1995, and CON #1265 dated 7 July 1995) against the updated content of the Databook. In the process of recording those issues which have been resolved, a new compilation of open items will be prepared. It is expected that the review of the Rev. 0 Databook will be completed by the end of October 1995. It must be noted that severe schedule compression exists due to the late delivery of the Databook. As a consequence, the capability to review the Databook in parallel with finalizing the LASEP-T analysis software is limited by available resources.

A replan of the entire safety analysis task was completed during this reporting period. The effort to properly handle variability and uncertainty was identified as an increase in work scope. Authorization was received from DOE to proceed with work on the variability and uncertainty subject matter as part of Task 8. (For consistency, efforts associated with treating analysis variability will be reported in this Task 3 section.)

During this six month reporting period, significant progress was made toward addressing the treatment of analysis variability and uncertainty. For both launch accident and reentry analysis efforts, lead engineers were appointed to this task. In addition through DOE support, experienced staff at Sandia National Laboratories were added to the analysis team. The assistance of Sandia, along with the continuing support from HNUS, has been essential in formulating the approach to treat analysis variability and uncertainty. As a significant program milestone, the approach for handling variability and uncertainty within the launch accident analysis was presented to INSRP 24 August 1995. For reentry variability and uncertainty, a working meeting was held between INSRP and the DOE analysis team on 28 September 1995. It is planned to present the final method for treating reentry analysis variability and uncertainty to INSRP at the end of October 1995.

Numerous review meetings were held with INSRP during this six month reporting period. A tabulation of the review meetings is provided below. These reviews which were agreed upon at the February 1995 PSAR review, are being held to provide the INSRP subpanels with current status of the analysis results and methodology. In general, the INSRP response to the content presented at the reviews has been generally favorable. The completion of these reviews is viewed as a significant accomplishment, especially in consideration of the schedule pressures to complete the FSAR work.

Safety Analysis Task
INSRP Reviews

No	Date	Review
1	20 April 1995	PSSP Review of LASEP-T Status
2	27 April 1995	RESP Review of Reentry CFD and Thermal Analysis
3	3 May 1995	MET Review of SPARRC Status
4	16 May 1995	BEES Review of SPARC Status
5	8 June 1995	Working Meeting with INSRP on Launch Accident Analysis Treatment of Variability and Uncertainty
6	10 August 1995	RESP Review of Reentry CFD and Thermal Analysis
7	23 August 1995	LASP Review of PSAR Comments and Databook Items
8	24 August 1995	INSRP Review of Launch Accident Analysis Treatment of Variability and Uncertainty
9	19 September 1995	Review Meeting with INSRP MET Chairperson
10	28 September 1995	Working Meeting with INSRP on Reentry Analysis Treatment of Variability and Uncertainty

Launch Accident Analysis

Detailed algorithms have been developed for the LASEP-T code. The following table identifies the models being developed for LASEP-T and the status of the models:

TOP LEVEL ANALYTICAL MODEL	SUBROUTINES	MODEL STATUS	REVIEW STATUS
Titan IV Time and Position Determination	GETMET	Complete	Complete
Blast Overpressure Generation	CBLAST	Complete	Complete
Blast Overpressure Assessment of RTG Projectile	OPRES	Complete	Complete
At-Altitude Fragment Generation - Centaur	CFRAG	Complete	Complete
At-Altitude Fragment Generation - SRMU	SFRAG	In Progress	FW-44
RTG Fragment Hit Evaluation	UHITIT	Complete	Complete
RTG Damage Assessment from Fragment Hit	FRGIMP	Complete	Complete
Trajectory Analysis / Ground Surface Determination	PMRK	Complete	Complete
RTG Damage Assessment from Surface Impact	SURFIMP	Complete	Complete
Space Vehicle Intact Impact Evaluation	SVIMPT	In Progress	Complete
Distortion Model	DST2REL	Complete	Complete
Fuel Release and Particle Size Distribution	FPSIZE	Complete	Complete
Buoyancy, Vaporization, and Coagulation	PUFF, FIREBALL	In Progress	FW-44

Integration and verification of the completed models has been initiated. The architecture for passing information between subroutines has been established.

Steady progress on RTG response hydrocode analyses continued at Orbital Sciences Corporation. Results have been forwarded as they have been completed and open lines of communication have been maintained to ensure that the proper priorities are being addressed.

Based on available expertise, it has been decided to have the vaporization and coagulation models developed at Sandia National Laboratories. Weekly telecons are being held to discuss progress. The aerosol physics model for the vaporization and coagulation portion is in progress. The buoyancy model is complete although a significant amount of integration between LASEP-T and SPARRC needs to be finalized.

Several INSRP review meetings were held during this period. Two meetings addressed the Lockheed Martin Astro Space position on the treatment of variability and uncertainty. Sandia personnel provided additional technical support. As a brief overview of the approach, it is planned to separate variability from uncertainty. The results of studies examining only variability are intended to reflect the expectation value, and the influence of uncertainty will then be examined to place confidence bounds on the expected value. The interface between LASEP-T and SPARRC and the overall process of calculating risk was also discussed. An additional meeting was held with INSRP's Power Systems Subpanel (PSSP) to discuss the algorithms and the overall approach to implement variability and uncertainty in the LASEP-T code to evaluate RTG response to launch accidents. Post meeting feedback indicated the INSRP Panel members were generally satisfied.

Internal LASEP-T model reviews were conducted to help classify model quantities as either variables (associated with variability) or parameters (associated with uncertainty). In addition, these reviews provided an opportunity for each of the responsible engineers to present their models and have model assumptions challenged and the overall modeling strategy discussed. The goal of these reviews was to have a consistent position on the treatment of variability and uncertainty and to obtain feedback from peers.

Reentry Analysis

Comparison with Ballistic Re-entry Vehicles

A large database on FWPF carbon/carbon performance in a high-temperature, high-loading environment exists from ballistic reentry vehicle (BRV) flight and ground test experiments. Although direct comparisons with the GPHS module cannot be made, because BRV nosetip shapes are generally not flat-faced like the GPHS module and differ in thickness and substructure, inferences about FWPF performance, relevant to the GPHS module, can be obtained.

Figure 3-1 shows the altitude time histories for the steep and shallow GPHS trajectories compared to a $\gamma = -40°$., high β, BRV trajectory. The ballistic coefficient ($\beta = W/C_DA$) of the BRV is about 100 times larger than the GPHS. As shown in Figure 3-1, the BRV for this case impacts about 20 seconds after reentry while the GPHS flight lasts several minutes. The Mach Number = 5 tick mark denotes, approximately, the last point on the trajectory where aeroheating is significant. The GPHS modules therefore have considerable time for thermal soak and cooling prior to impact, while the BRV maintains a high heating rate to impact.

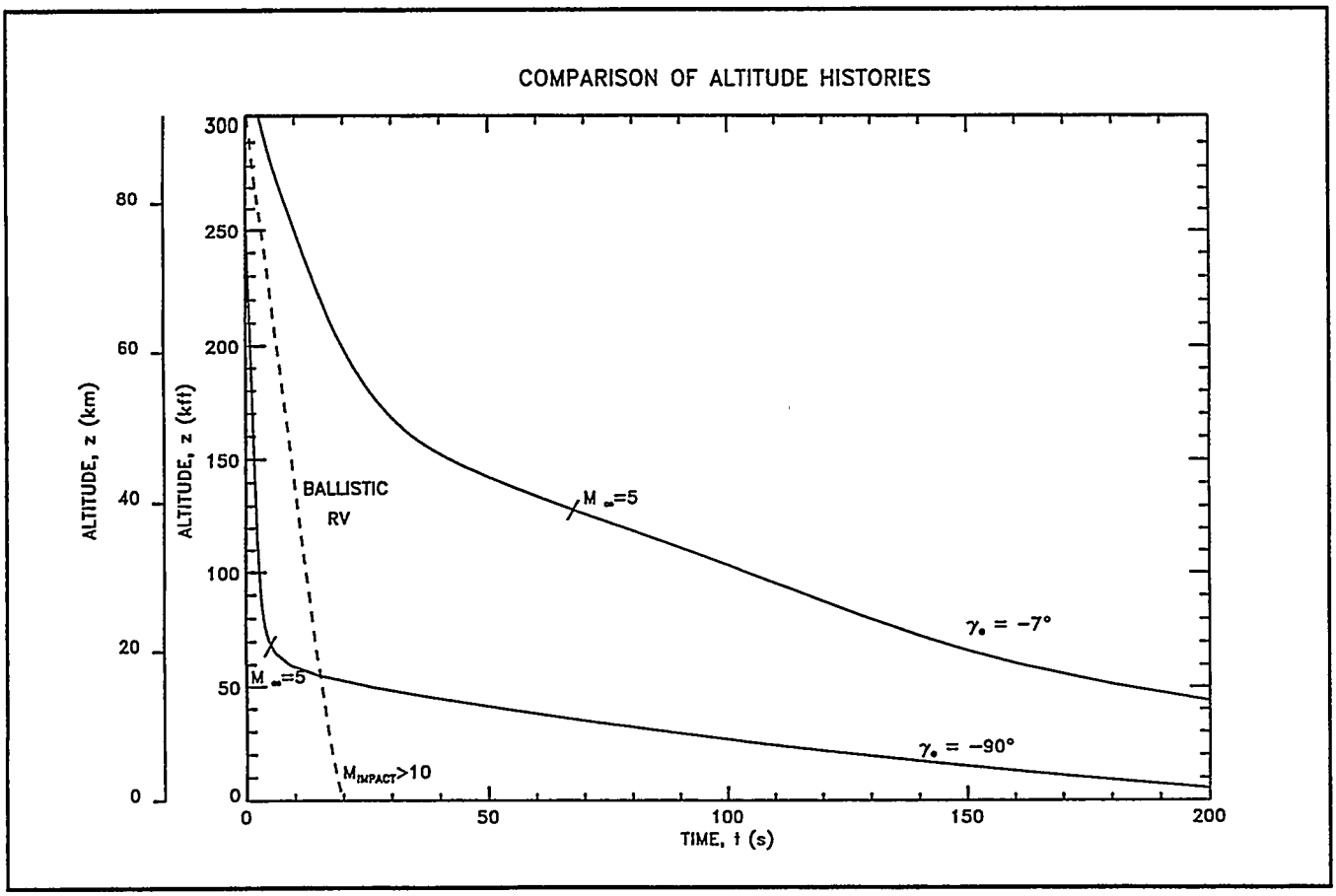

Figure 3-1. BRV Heating to Impact. GPHS Long Cooling Period Prior to Impact

Figure 3-2 compares the dynamic pressure experienced by a BRV and the GPHS. Because the BRV maintains a high velocity in the dense low altitude regime, the peak q approaches 100 atm. The worst case for the GPHS is an order-of-magnitude smaller q because its velocity decay occurs at much higher altitudes.

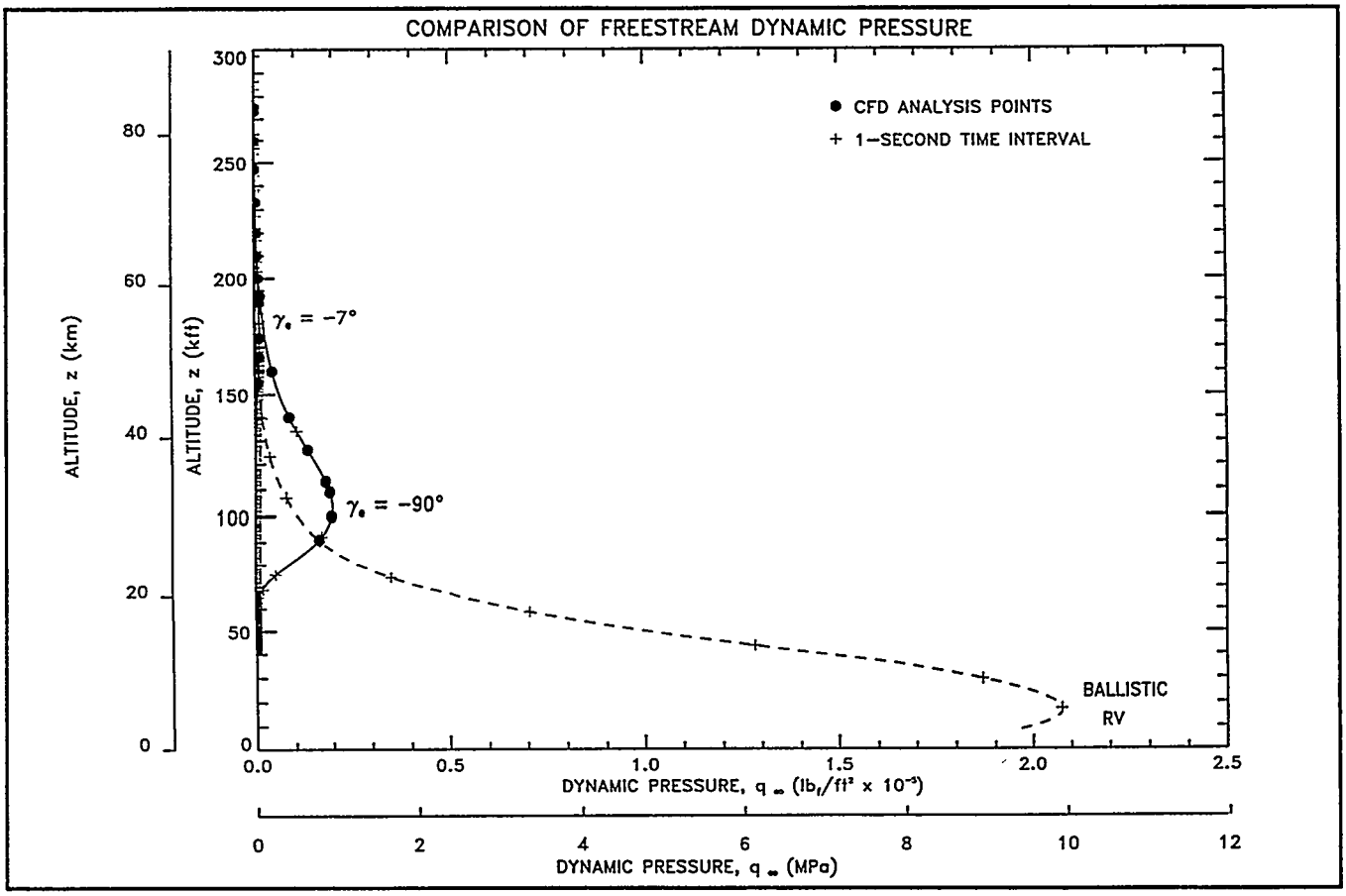

Figure 3-2. BRV Peak Dynamic Pressure (~100 ATM) Is 10X GPHS Worst Case

The inertial loads, shown in Figure 3-3, are severe for the GPHS (steep trajectory) compared to a BRV. The rapid slow down of the GPHS leads to over 1000 g's while a BRV, and the shallow trajectory GPHS, experience a peak of about 100 g's. The thermostructural response to the 1000 g load will be analyzed in detail. However, experimental launches from high velocity guns have shown that unheated carbon/carbon nosetips can withstand loads of over 50,000 g's.

Transition from laminar-to-turbulent flow over the BRV nosetip occurs at about 40kft. While transition correlations for the flat face GPHS module do not exist, the peak Reynolds number (based on diameter) is two orders-of-magnitude less for the GPHS. This suggests that the flow over the GPHS front face will remain laminar.

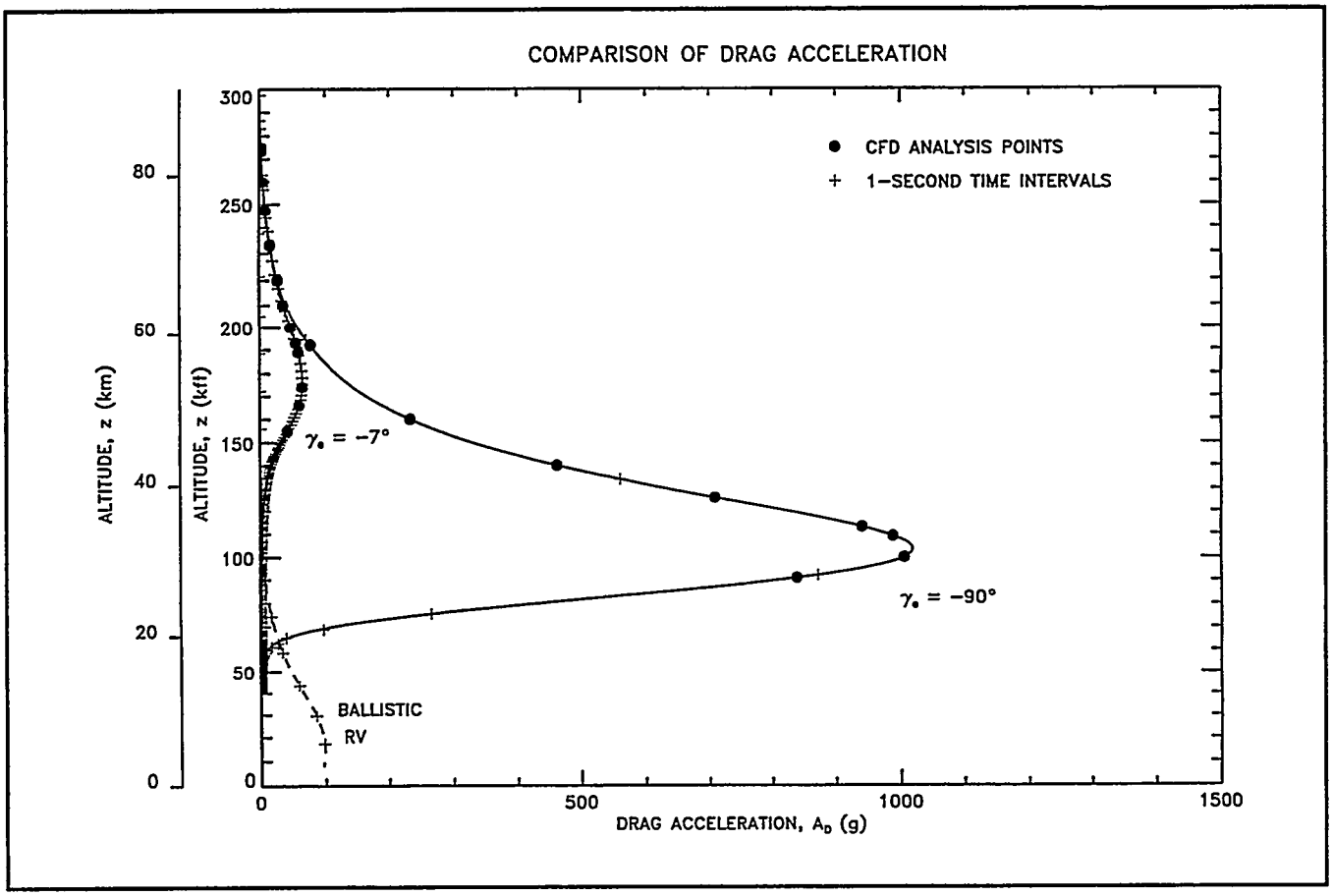

Figure 3-3. GPHS (γ = 90°) Peak g Load Is 10X BRV Peak

The predicted stagnation point temperature history for the BRV is shown in Figure 3-4. The transient heating prediction technique is tailored to BRV spherical nosetips and environments and has been calibrated with flight data. As shown in Figure 3-4, peak surface temperatures approach 4500°K. At the time of peak temperature, nosetip stagnation point pressure is also peaking at about 184 atm.

The equilibrium sublimation behavior of carbon, as a function of temperature and pressure, is shown in Figure 3-5. The B' axis is a non-dimensional ablation rate. The maximum temperature and pressure point for the BRV nosetip is shown as well as the GPHS steep trajectory peak pressure isobar. The isobar curves show that a high pressure is needed to sustain a high wall temperature. The inference is that the worst case GPHS pressure, an order-of-magnitude less than the BRV pressure, will not support the high temperatures that are possible on a BRV nosetip.

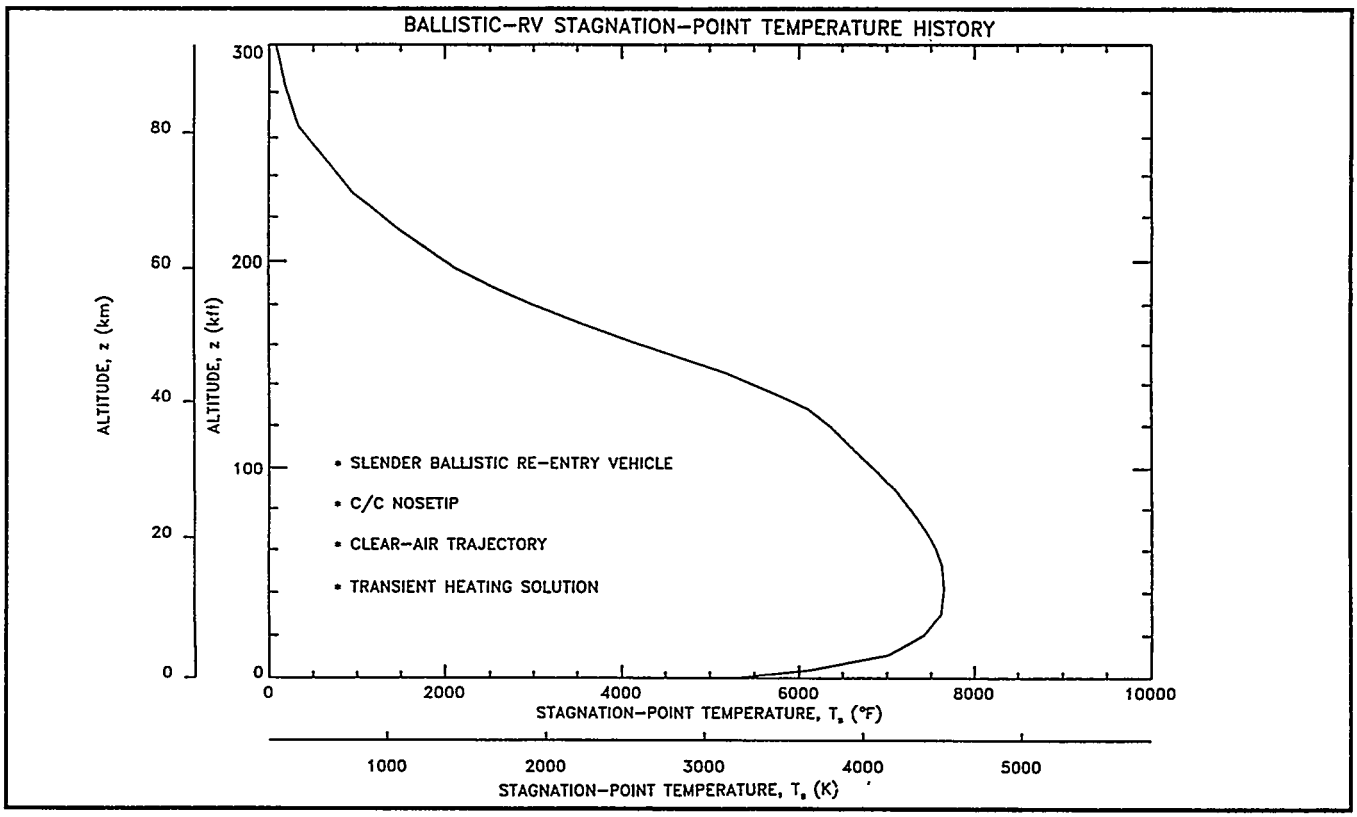

Figure 3-4. Peak BRV Temperatures Approach 4500°K (7640°F) at 100 ATM

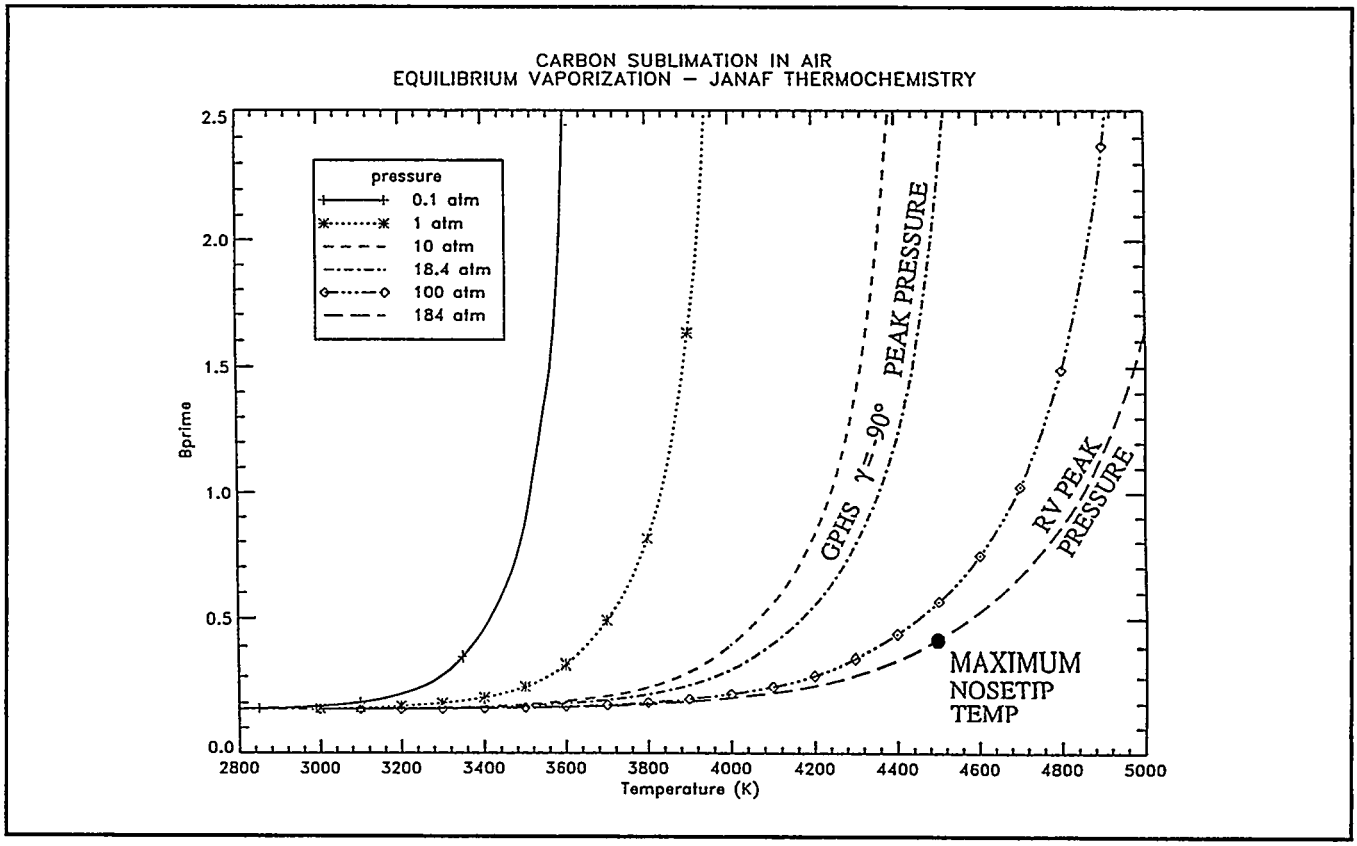

Figure 3-5. BRV Nosetip Maximum Temperatures May Exceed GPHS Worst Case

Comparisons with BRV trajectories show that BRV nosetip temperatures and pressures exceed those expected for the GPHS; and BRV nosetips survive. However, recession on BRV nosetips is typically measured in inches while the FWPF thickness for the GPHS is only about 0.19 inches. The critical issue is therefore not if FWPF material can survive, but if is there sufficient margin in the thickness of the heat shield.

Completion of the RACER Flowfield Code

A new Navier Stokes flowfield code was developed to overcome the limitations of the LAURA code. LAURA was initially selected for reentry analyses of the GPHS modules because of its demonstrated capabilities and its coupling with the LORAN radiation code. However, in practice, LAURA proved to be very slow to converge and difficult to extend to new flow regimes, such as low altitude near equilibrium conditions. A new technique was needed that could be applied across the entire range of altitudes and velocities (approximately one hundred cases) and yet require only a fraction of the computational resources consumed by LAURA.

The new Reacting, Ablating, Chemical Equilibrium/nonequilibrium with Radiation (RACER) full Navier Stokes code has proven to converge better than an order of magnitude faster than LAURA and successfully compute flows ranging from the high altitude slip flow regime down to high Reynolds number equilibrium conditions. Several extensions and improvements of the RACER algorithm were developed to obtain this capability. These extensions, described below, are now complete and RACER is being applied, in parallel with SINRAP, to compute the thermal response of the GPHS along the shallow trajectory.

Modifications for High Altitude

The initial trajectory point for CFD analyses is at an altitude of 83.3 km (273 kft). At this altitude the environment, with a Knudsen number of 0.1 (based on a 100mm characteristic length), is well into the transitional flow regime. Previous Navier Stokes analyses by Gnoffo (Gnoffo, et al., 1989) and others have shown fairly good agreement with Direct Monte Carlo Simulation (DMSC) techniques in this regime. The validity of the Navier Stokes solution is enhanced by a bow shock capturing approach (rather than shock fitting) which accounts for "shock slip" effects. However, this case is computationally difficult for most, if not all, Navier Stokes solvers. Extensions to the new flow solver that have been devised to alleviate numerical problems and treat high altitude phenomena are summarized below.

Thermochemical Modeling: The extreme shock layer temperatures for this case (up to 55,000°K) were significantly beyond the range of the thermodynamic and reaction rate database. The current thermodynamic data, based on the curve fits of Gupta et al. (1991),

were extrapolated using a constant specific heat approximation. The high temperature reaction rates were initially addressed by incorporating the concept of a "rate limiting temperature" (Gnoffo et al., 1989, and Park et al., 1994). More recently, a new point implicit thermospecies coupling was developed to address the strong dependence of the reaction rates (particularly the electron impact reactions (EIR)) on the local temperature. This thermospecies coupling permitted the scheme to treat temperatures as high as 60,000°K without stability problems. Consequently, the value of the rate limiting temperature was raised to 60,000°K, which is above any temperature encountered in the flowfield.

Grid and Solution Stability: At this high altitude condition the bow shock is no longer a sharp discontinuity. The shock layer is very thick and pressure and temperature gradients do not coincide. This caused problems with the algorithm that locates and adapts the grid to the evolving outer boundary. The outer boundary scheme, which was based on shock normal Mach number, was changed to a pressure gradient approach. This resulted in a stable adaptation of the grid to the flowfield and captured both pressure and temperature gradients. The number of streamwise points was reduced from 45 to 35 by adjusting the grid clustering in the vicinity of the corner. This improved stability and reduced computational time without any noticeable loss of accuracy.

Inclusion of a Carbon Ablation Model

The CFD wall boundary condition imposes a specified T_{wall} based on SINRAP transient heating analyses. The wall ablation model is based on the Knudsen Langmuir relation (Baker, et al., 1977) and consists of the following steps:

(i) Predict the element composition at the wall using the element conservation equations and the mass balance of element convection and diffusion.

(ii) Predict the species composition at the wall using the predicted element composition and the assumption of equilibrium catalytic wall conditions.

(iii) Use the specified wall temperature, the predicted pressure and species composition, and the Knudsen Langmuir relations to compute the wall ablation rate.

Wall Catalysis Modeling

An improved equilibrium wall modeling capability was developed for the carbon air system. The new model requires a larger matrix but is more stable and converges faster.

Extensions for Equilibrium Chemistry

The final extensions of the new flow solver, needed prior to putting this code into production, addresses the equilibrium and near equilibrium regimes and the treatment of fast reactions. The new code utilizes the element conservation equations, rather than just

the species conservation equations (as in the LAURA formulation). This approach provides a much better means to alleviate the "stiffness" problem that occurs at the lower altitude, equilibrium flow, trajectory points. A new wall boundary condition scheme has been devised based on a constant Lewis number for element diffusion (while retaining a variable Lewis number for binary diffusion). This scheme overcomes the very slow convergence of the wall chemistry in LAURA (that compounds the already slow convergence of the code). Test cases were performed to check these modifications and to verify the code's equilibrium capability. Trajectory points on the low altitude portion of the steep trajectory were selected. The flowfield readily converged for the test cases at 125kft and 100kft. The solutions agree with the expected equilibrium flow behavior.

Completion on the LORAN C Radiation Code

The LORAN code was extended under the previous study to carbon species. This new version of the code was named LORAN C. In this study the efficiency of the code was greatly improved, some minor FORTRAN errors were corrected, and the code was ported to an HP 735/125.

Development of a LORAN C Pre-Processor

The new flowfield code's output had to be converted to a LORAN C flowfield input file (as had been done for the LAURA C flowfield code). A pre-processor was written to compute cell centered flow values given flow variables at the grid points (recall that the new flow solver is a finite difference technique whereas LAURA employs a finite volume approach). In addition, the output of the new flow solver was manipulated to obtain variables, units, and non-dimensionalizations consistent with LORAN.

LORAN Run Time Improvements

With the vast improvement in run time offered by the new flow solver (compared to the original LAURA C code), the LORAN C radiation code became the limiting factor in analysis turn around time. Efforts therefore focused on reducing LORAN times in order to accomplish the extensive case matrix. The LORAN C code, extended to include a 19 species carbon air model, requires about six hours CPU time on the SUN SPARC 10. With approximately one hundred cases to compute, and each case requiring several applications of LORAN C in the global iteration process, a goal was established to reduce the LORAN C run time by a factor of six. The run time was first reduced from six to five hours by switching to a SUN SPARC 20. A further reduction, with minimal code changes, was obtained by employing the SUN's FORTRAN optimizer. The maximum level of optimization yielded two-hour run durations.

LORAN C was converted to the HP 735 so that a common platform could be used for the flow and radiation codes. Because the HP FORTRAN compiler is far more rigorous than the SUN, numerous changes were needed to obtain a successful HP version of LORAN C. The initial HP code runtime was comparable to the optimized SUN version. Experiments with the numerous options in the HP FORTRAN optimizer, however, led to a substantial reduction in run time. The "production" version of LORAN C is now reduced to 40 minutes CPU run time. A net factor of nine decrease in run time has been achieved.

Resolution of Errors in LORAN

Flux Divergence: The divergence of the radiation heat flux appears as a source term in the flowfield energy equation. This term is computed in LORAN using a three point central difference formula on a unequally spaced grid; except at the wall boundary where a one sided, three point difference formula is necessary. It was discovered that there was a sign error in this one sided formula in the original LORAN code. The error probably escaped detection because the near wall cell, at low temperature compared to the region near the bow shock, has only a minor affect.

Spurious Radiation: The LORAN C solution for the first trajectory point (highest altitude), low wall temperature case, failed in the low temperature region above the shoulder of the GPHS module. LORAN is known to have difficulties when the flow temperatures are low. Because of this problem, a technique had been incorporated in the original LORAN code to exclude freestream points. However, for this case, low temperatures occur in the shock layer and spurious molecular emissions are computed. The LORAN C solution for the third trajectory point, high wall temperature case, displayed severe oscillations between iterations that could not be attributed to the changes in the flowfield during the global iteration process. In this case, large molecular emissions were being incorrectly computed when certain species concentrations became extremely small. Both of these problems were resolved by filtering the RACER computed concentrations to impose a small, but finite, concentration level for LORAN C computations. Test cases were performed to verify that these trace concentrations did not alter the computed radiation field.

Shallow Trajectory Analyses

The "production" process to accomplish the approximately one hundred coupled flowfield/radiation cases was initiated for the shallow trajectory. Each flowfield/radiation case requires global iterations of the RACER and LORAN C codes. Typically four to seven passes are sufficient to obtain converged heat flux and ablation rate distributions. The solution process is shown schematically in Figure 3-6. At each selected trajectory point, three globally converged solutions are obtained. Each solution uses a specified wall

temperature based on the SINRAP transient wall temperatures at a previous trajectory point. As shown in Figure 3-6, the solutions at three trajectory points form a nine-point stencil for interpolation in SINRAP of the wall heat flux, enthalpy, and ablation rate. To expedite the computational process, a procedure has been developed to run LORAN for all nine cases simultaneously on nine SUN SPARC 20 Workstations. In addition, the RACER computations are performed in parallel on two HP 735/125 Workstations. Although the HP version of LORAN is twice as fast as the SUN version, the availability of nine SPARC 20's more than compensates for the single machine disadvantage. Use of the SUNs also frees the HPs for the RACER analyses.

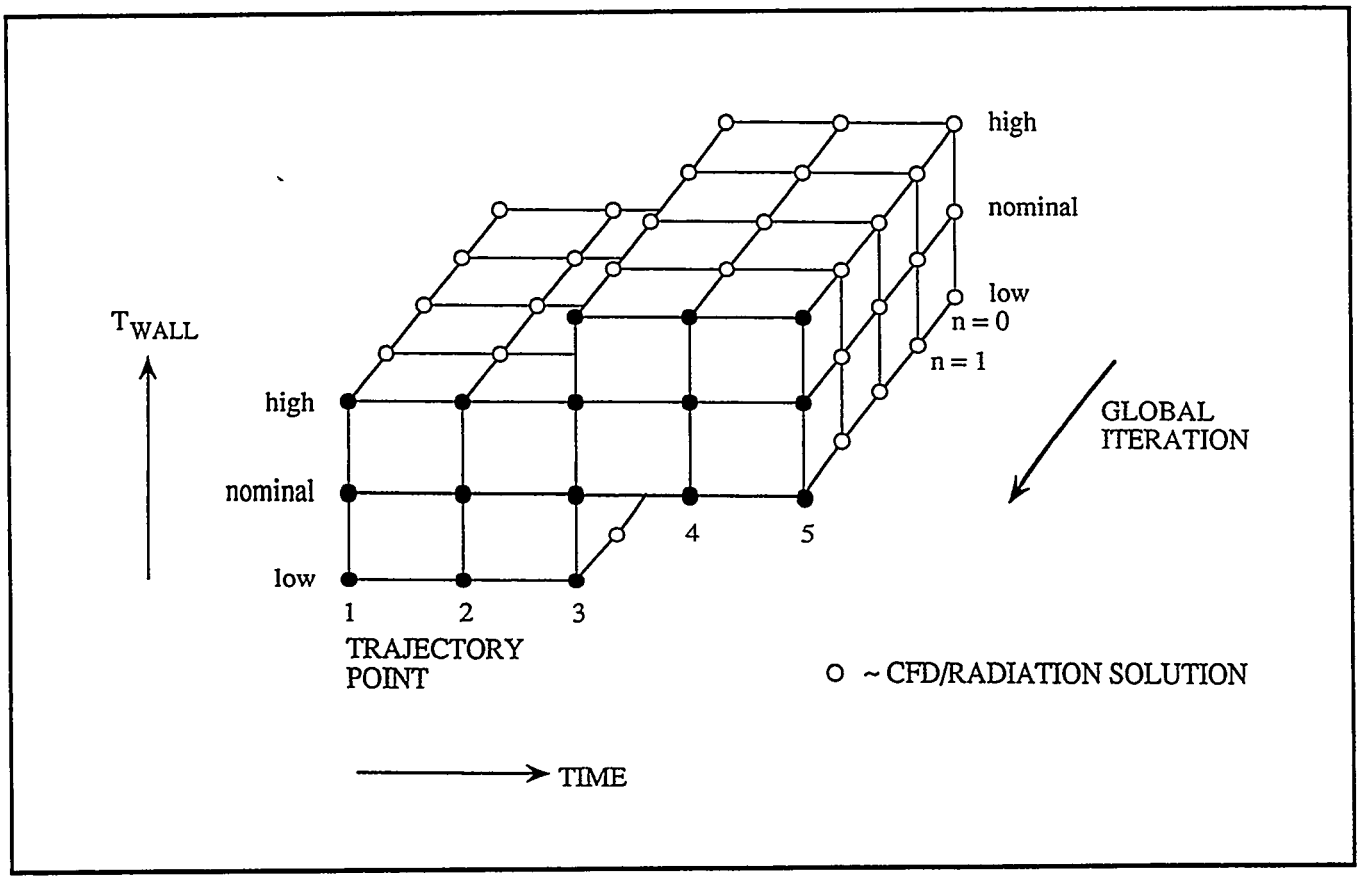

Figure 3-6. Schematic of CFD/Radiation Computational Matrix

Results

Globally converged solutions have been obtained for the first five (out of a planned ten) points on the shallow trajectory. These points, shown schematically in Figure 3-6, comprise two nine-point stencils for SINRAP. The specified freestream conditions and front and side wall temperatures are shown below in Table 3-1

Table 3-1. Initial Cases for the Shallow Trajectory.

Altitude (Ft)	Velocity (Ft/Sec)	T_{wall} (° R)	
		Front	*Side*
273,219	65,190	5160	3060
		5760	3710
		6360	4360
259,936	64,965	5160	3060
		5760	3710
		6360	4360
247,344	64,540	5160	3060
		5760	3710
		6360	4360
224,381	62,643	5760	3710
		6360	4360
		6860	4860
204,690	58,571	5760	3710
		6360	4360
		6860	4860

Each case is first globally converged on a "coarse" 35x35 grid. Grid sensitivity is then tested by employing a "fine" 51 (body-to-outer boundary) x35 (along the body) grid for selected cases. These tests have shown that a 35x35 grid, for the first five trajectory points, matches all wall properties (for SINRAP) of a 51x35 grid to within 2%.

Solution trends with altitude are shown in Figures 3-7 to 3-12. Figure 3-7 shows the surface pressure distribution for five altitudes, all with a front face temperature of 6360°R and a side wall temperature of 4360°R. At 205kft, the pressure load on the front face has increased to almost eighteen times the level at high altitude (273kft).

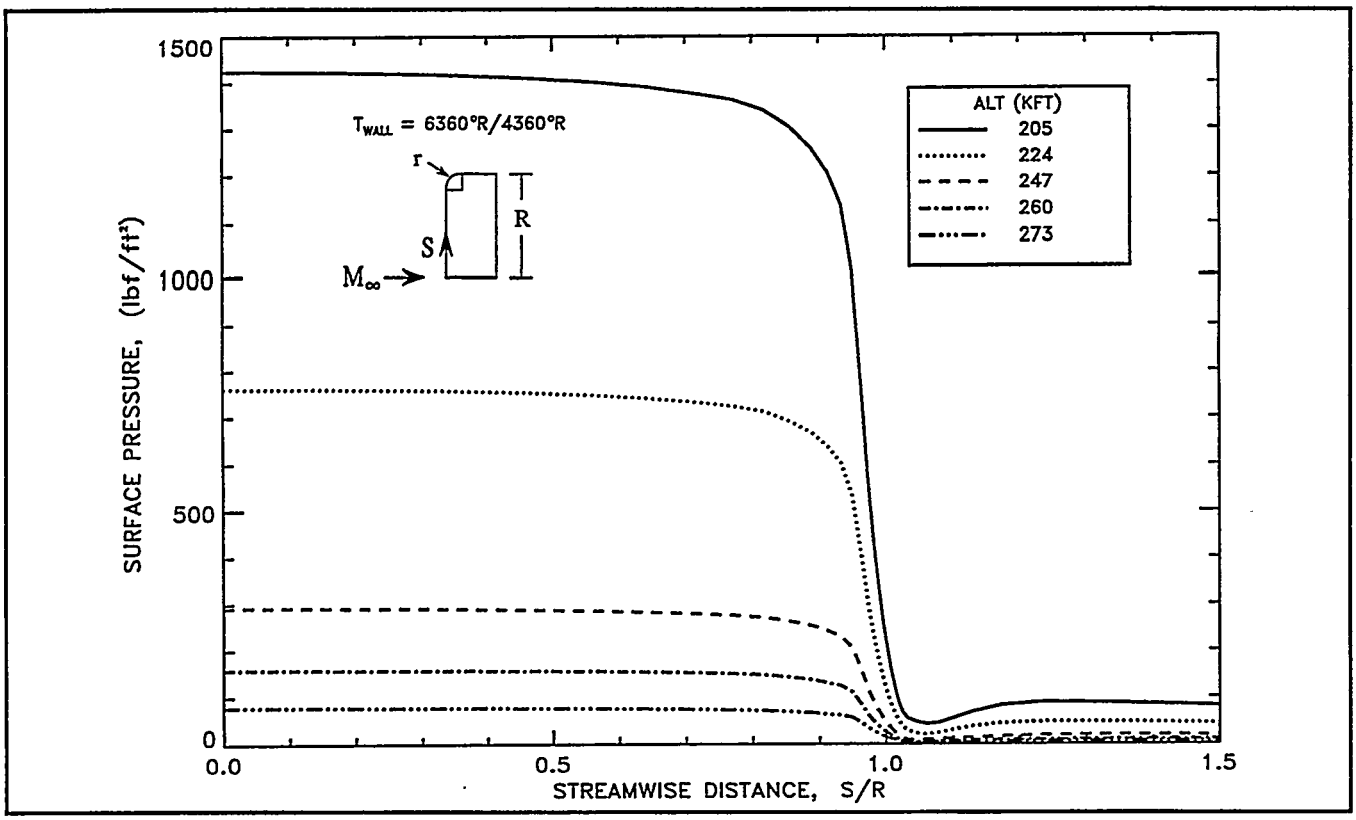

Figure 3-7. Surface Pressure History (Shallow Trajectory)

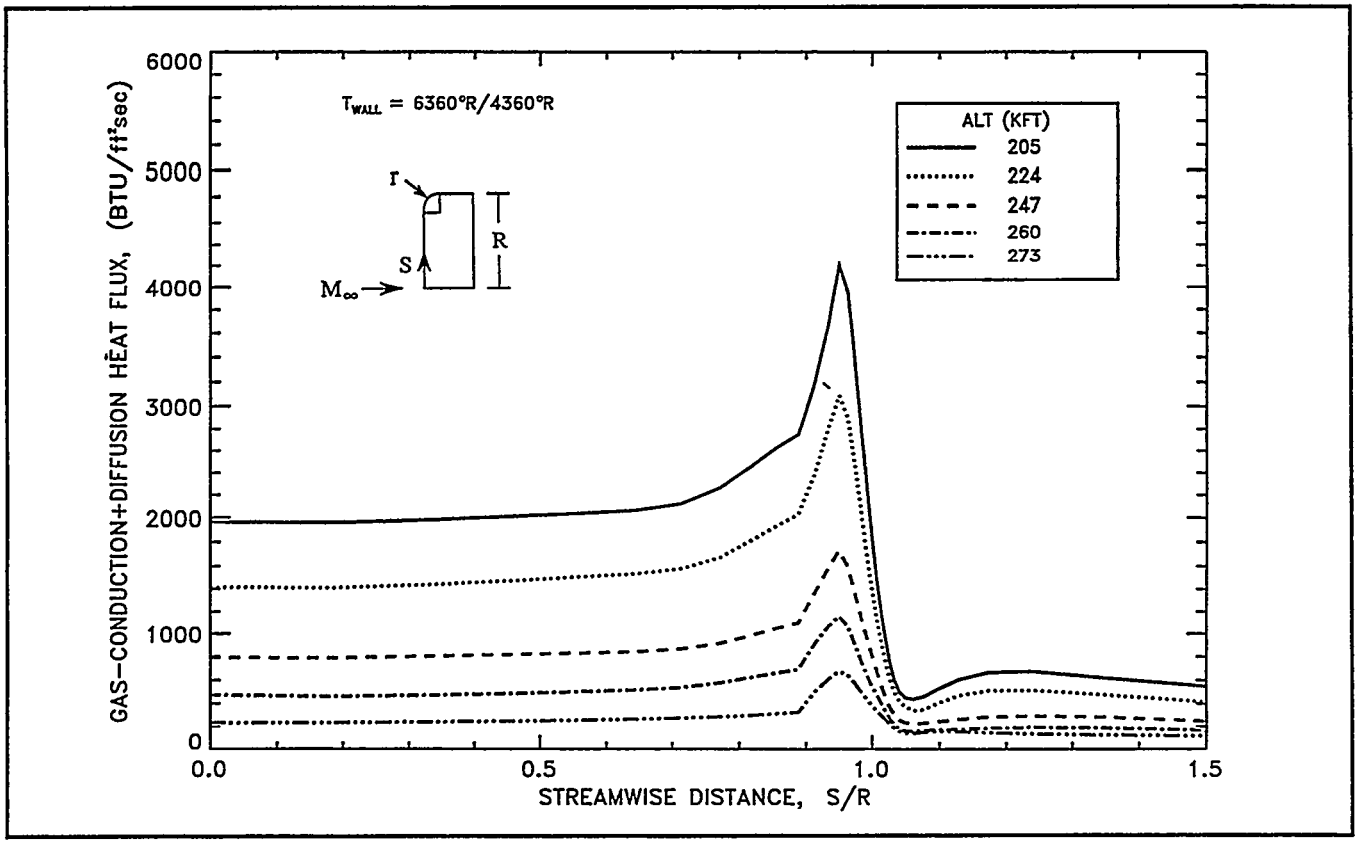

Figure 3-8. Surface Gas Conduction Diffusion Heating History (Shallow Trajectory)

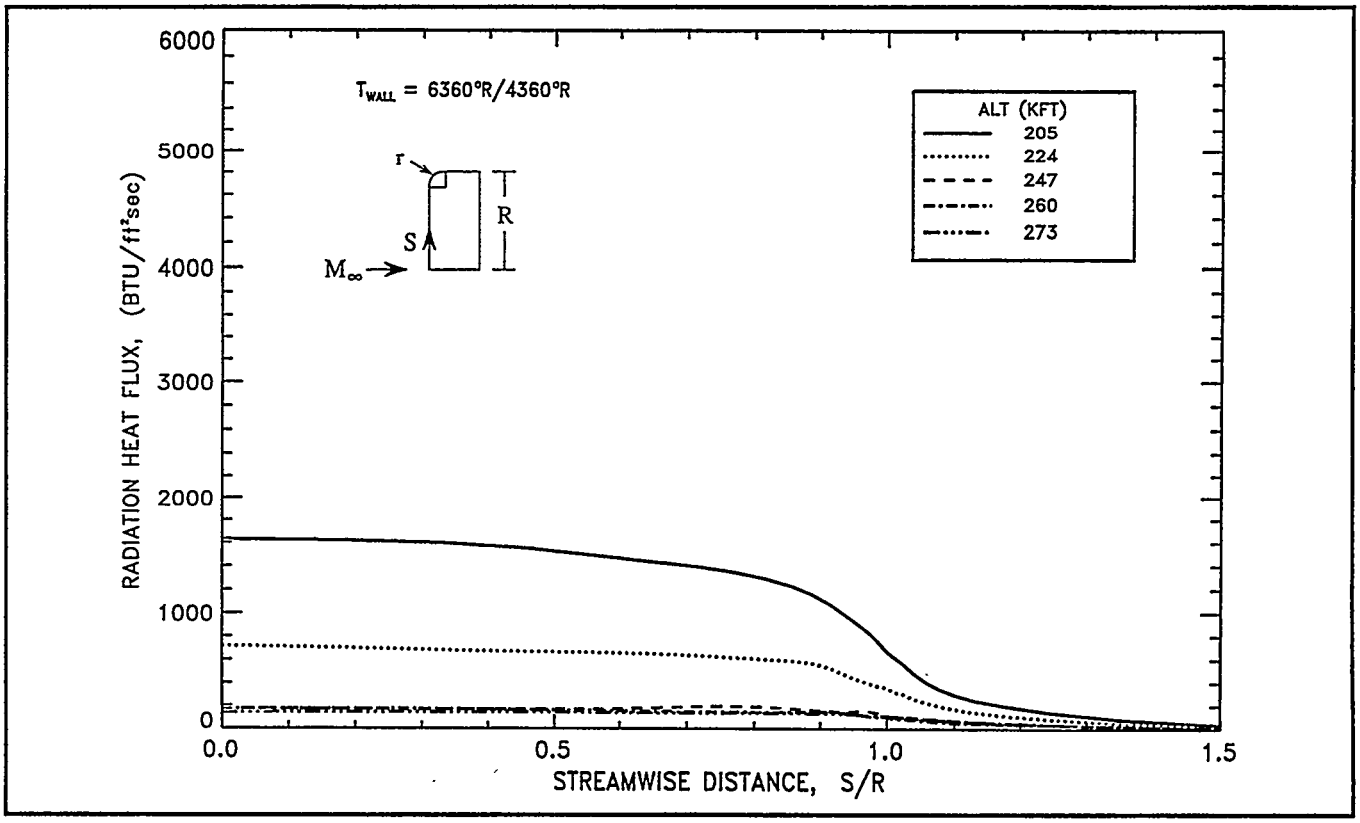

Figure 3-9. Surface Radiation Heating History (Shallow Trajectory)

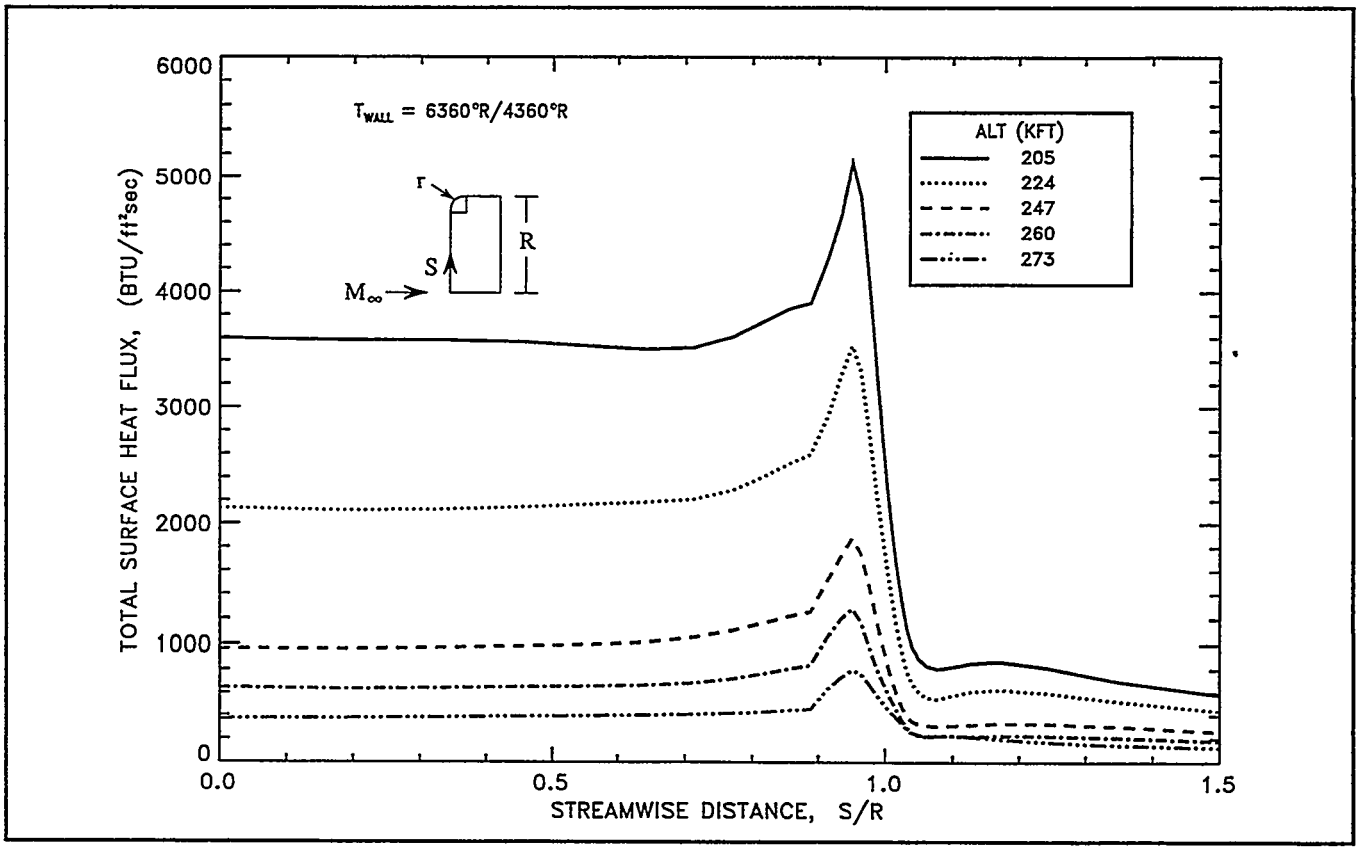

Figure 3-10. Surface Total Heat Flux History (Shallow Trajectory)

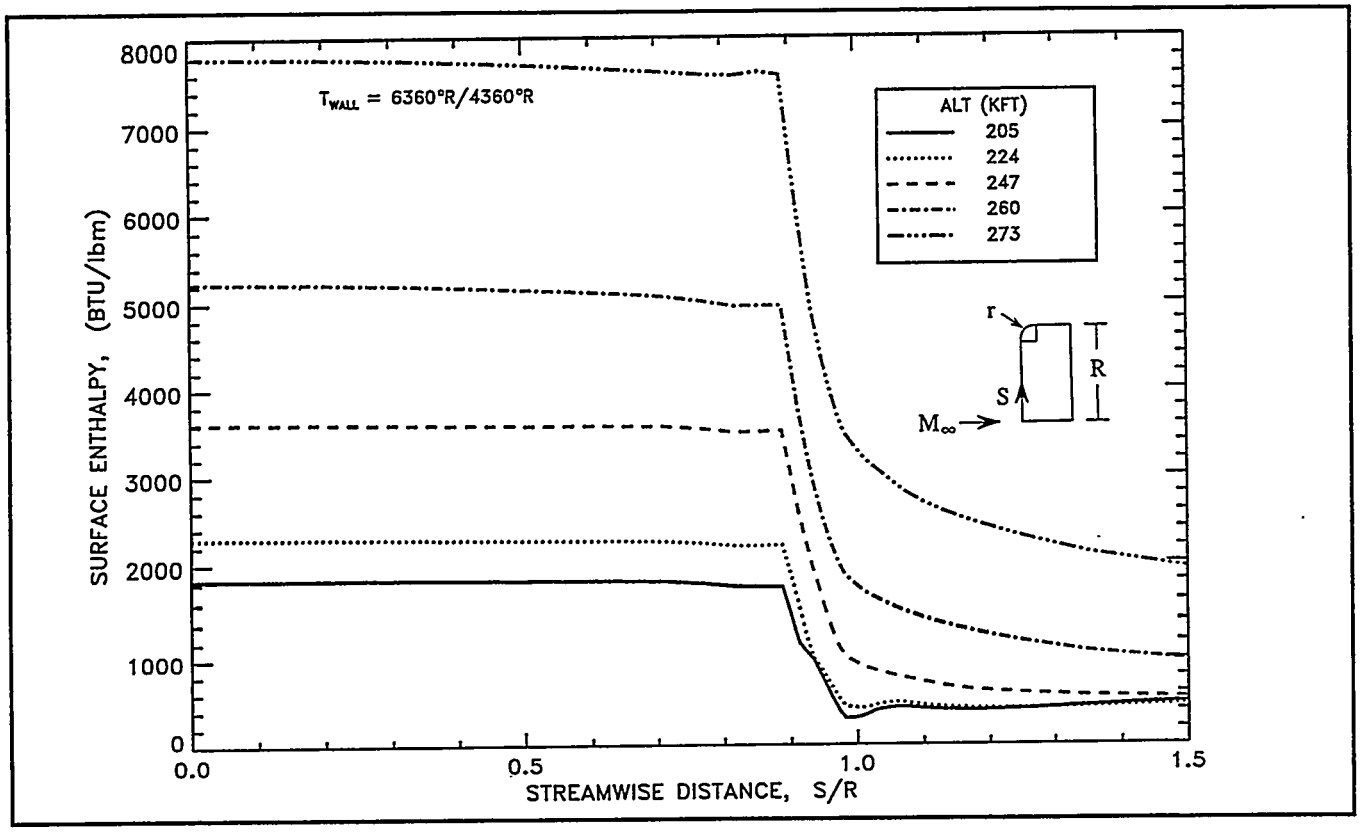

Figure 3-11. Surface Enthalpy History (Shallow Trajectory)

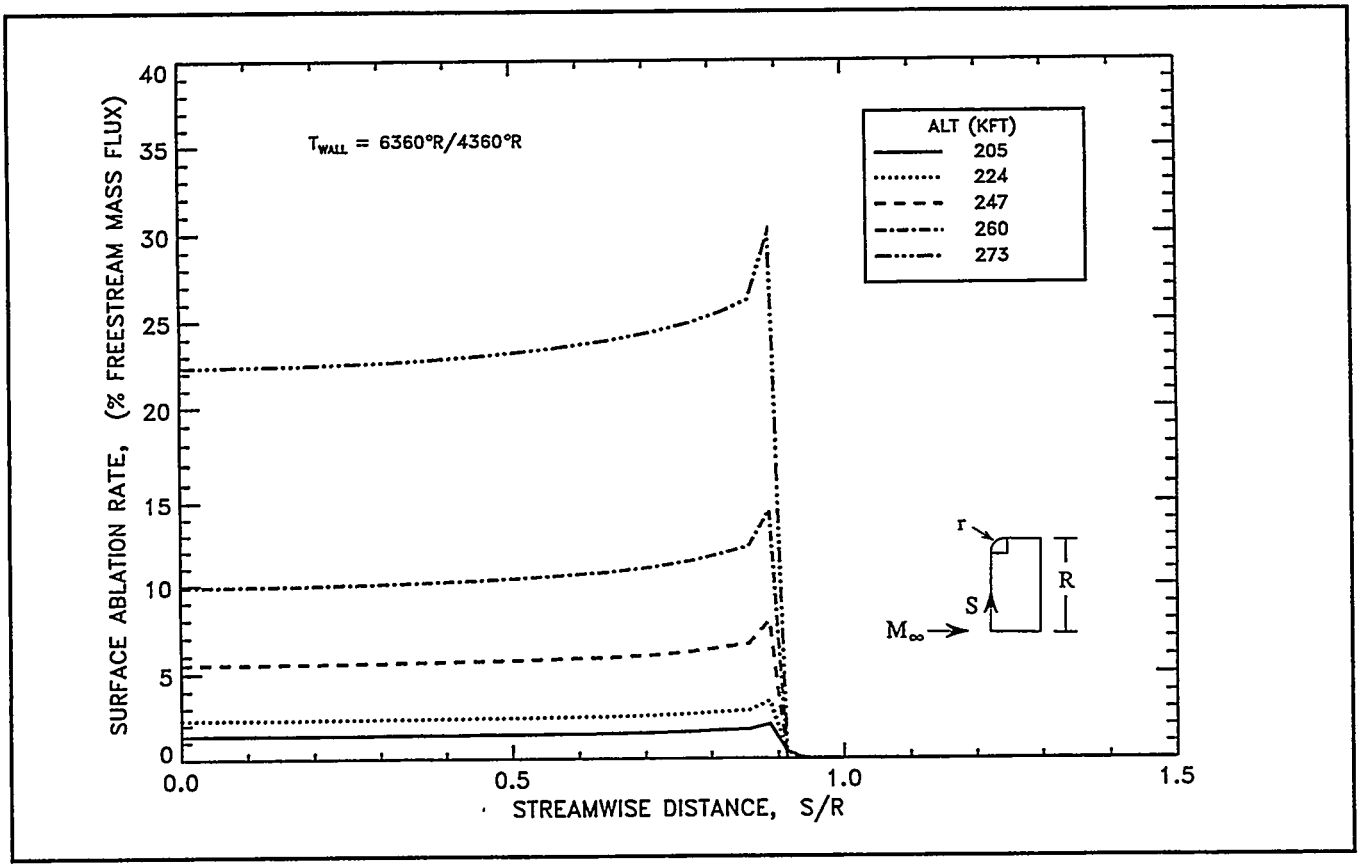

Figure 3-12. Surface Ablation Rate History (Shallow Trajectory)

Figures 3-8 to 3-12 show the terms used in computing the surface energy balance in SINRAP. The gas conduction + diffusion heat flux surface distribution is shown in Figure 3-8. This heat flux term has increased, by a factor of nine, from its high altitude value. The large peak in heat flux at the corner is due to both small radius effects and the drop in wall temperature (a linear drop from the front to the side wall is imposed). The radiation heat flux, shown in Figure 3-9, increases at lower altitudes by a factor of five. Figure 3-10 shows the corresponding total heat flux distribution. The gas enthalpy surface distribution, Figure 3-11, falls by a factor of four from its high altitude level. The ablation rate as a percentage of the freestream mass flux, Figure 3-12, drops dramatically with altitude. The "spike" at the corner is due to the pressure drop over the rounded edge.

Work in Progress

The RACER and LORAN C codes are now in production and work on the shallow trajectory is proceeding in step with SINRAP. The selection of wall temperatures and freestream conditions for future cases is dependent on SINRAP results. In addition, the selection of future cases may require iteration between SINRAP and the CFD/radiation case matrix because of the sensitivity of the terms in the surface energy balance to the wall temperature.

Thermal Analysis

On 27 April 1995, a meeting was held at the Building B facility in Valley Forge with members of the INSRP RESP (Reentry Subpanel). At this meeting presentations of the CFD analysis work and the SINRAP modifications made to utilize CFD results were made. The purpose of these presentations was to provide an update to the panel on the plans to perform reentry analyses. Previous comments from the RESP subpanel including PSAR comments were also discussed.

As discussed in Figure 3-6 of the CFD section, the strategy for incorporating CFD results into SINRAP is to perform CFD runs over a range of constant front face temperatures for individual pre-selected trajectory points. Iterations will then be performed within SINRAP by obtaining the appropriate CFD parameters as a function of both 1) time (velocity and altitude) in the trajectory, and 2) current surface temperature. Iterations at each time step in the SINRAP reentry thermal analysis will proceed until a heat balance is obtained for all nodes.

Past SINRAP results for Cassini, obtained using the former analysis method without CFD input, will be used to initially select the range of surface temperatures for the CFD runs. While the former results for the shallow case for the face-on-stable orientation showed fairly uniform surface temperatures on the front face, the steep case had a surface temperature variation of 500°F. Because of this input, it was deemed necessary to explore if the CFD results for steep trajectories can be used by SINRAP when the CFD runs are made with uniform (or constant) front face surface temperatures. Therefore, it must be determined if CFD computed heat flux and ablation rates are a function of local wall temperature (and pressure) or if CFD results are influenced by cumulative effects of upstream ablation and gradients in wall surface temperature.

To evaluate this matter, CFD output was obtained for two test cases, each having the same wall temperature at a defined distance from the stagnation point (S/R = .88). One case had a fixed wall temperature for all front face nodes; the other case had a variable or non-constant wall temperature which decreases from the stagnation point to the surface edge. These imposed temperature profiles are shown in Figure 3-13. The test cases were run at the altitude and velocity corresponding to peak heating conditions for the shallow entry angle (-7°). The constant front face surface temperature level is consistent with the former SINRAP results for the shallow case, and the imposed non-constant wall temperature profile is analogous to the temperatures computed for the steep case. The common temperature point was placed near the corner where gradients are the most severe and where the largest accumulation of the convected carbon species occurs.

The LAURA-C flowfield and LORAN-C radiation codes were applied in a global iteration procedure. The LAURA-C code was used to generate the flowfield data needed by LORAN-C. The LORAN-C code, in turn, provides a corresponding radiation field for the next pass with LAURA. For the test cases, it was attempted for the first time, to drive the global iteration process to tight convergence. In this effort (with initial unconverged results presented at the RESP 27 April 1995 meeting) successive applications of LAURA/LORAN were monitored. Convergence was found to be quite slow so a relaxation procedure for the radiation solution was devised. The previous two radiation field solutions were averaged with the current solution and used as the updated radiation field for LAURA. This approach was found to accelerate the global-convergence process.

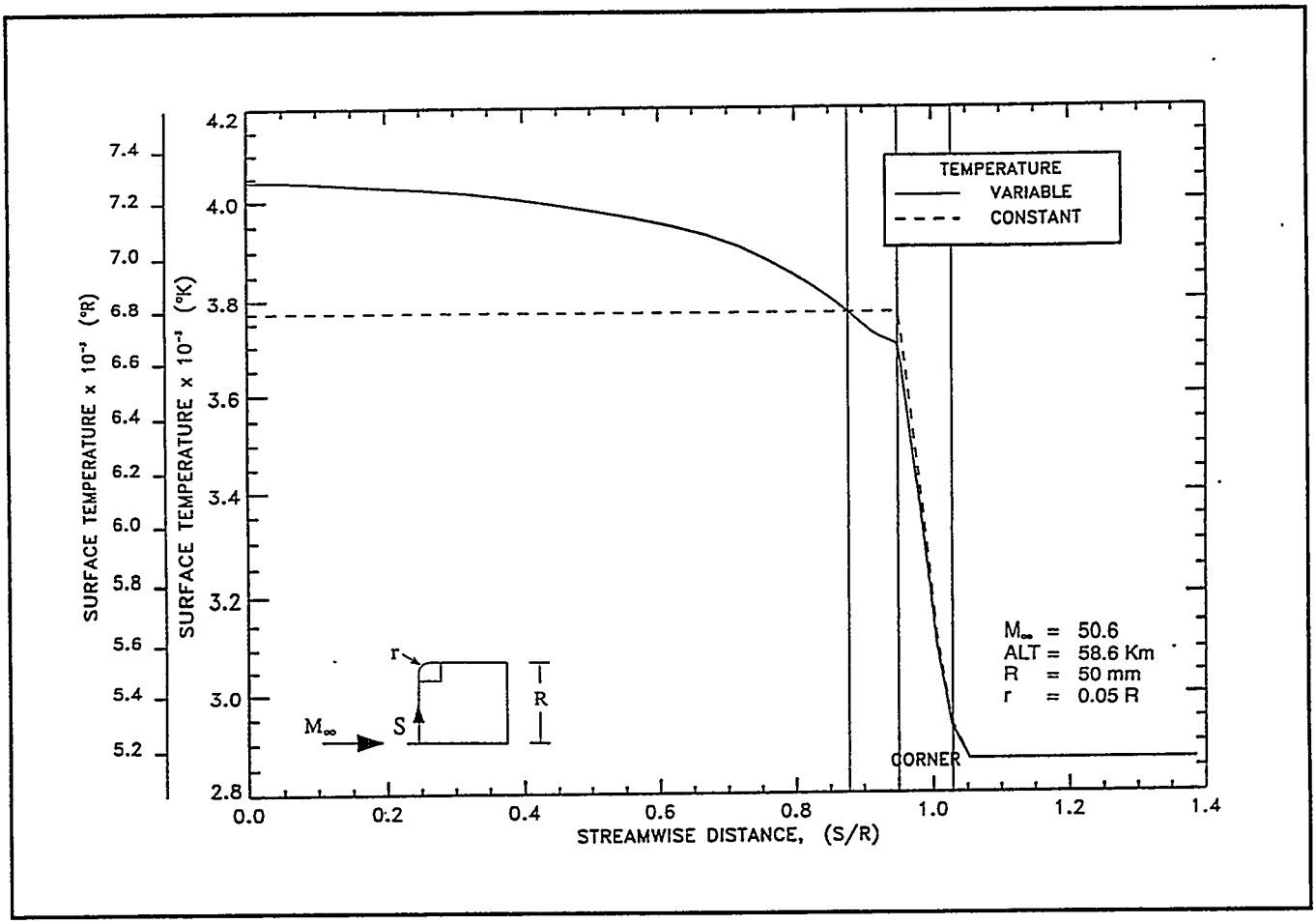

Figure 3-13. Imposed Wall Temperatures for CFD/SINRAP Test Cases

Figure 3-14a shows the global-convergence history of the surface pressure distribution for the non-constant wall temperature test case. For this case, as expected, radiation has almost no influence on pressure so that the initial LAURA-C(0) solution does not change with subsequent global iterations. The convergence history of the heat flux components is shown in Figure 3-14b (gas conduction and diffusion) and 3-14c (radiation). The gas conduction plus diffusion heat flux components increase during the global iteration process in response to the decrease in surface ablation rates, shown in Figure 3-14d.

The final, globally converged, heat flux components for the variable wall temperature case are shown in Figure 3-15. Radiation dominates in the stagnation region but the gas conduction plus diffusion heat flux component rises sharply across the front face and dominates near the 0.05R radius corner. The total heat flux peaks on the front face near the tangency point of the rounded corner.

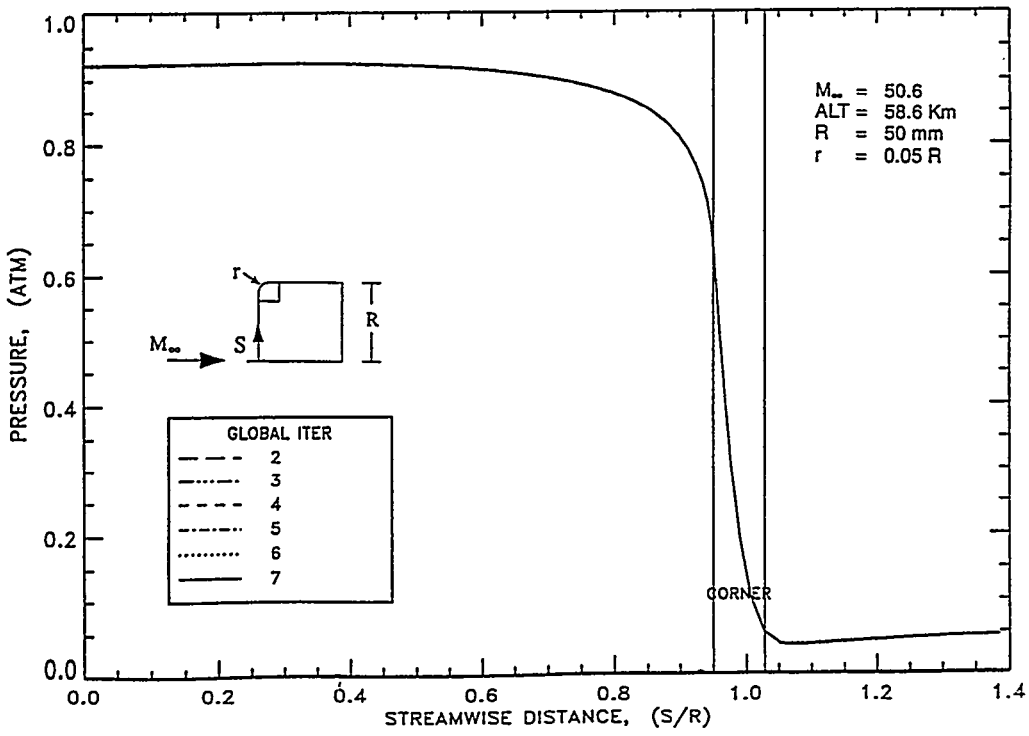

(a) Surface pressure convergence

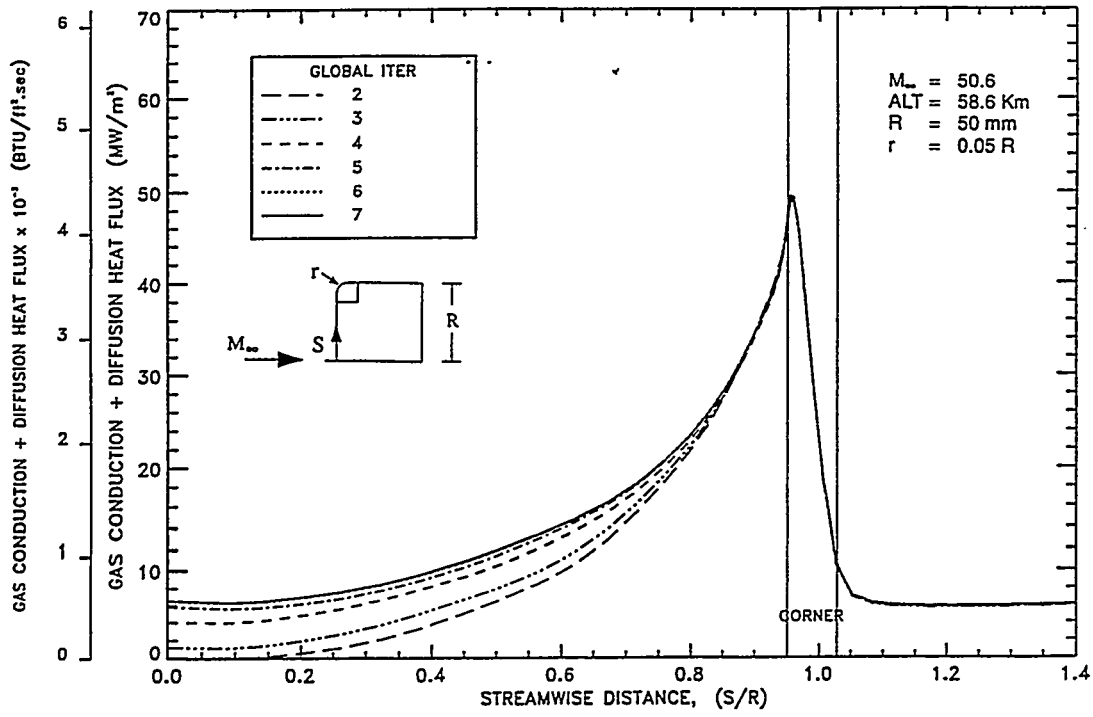

(b) Gas conduction plus diffusion heat flux convergence

Figure 3-14. LAURA - LORAN Global Convergence History for Variable Wall Temperature Test Case

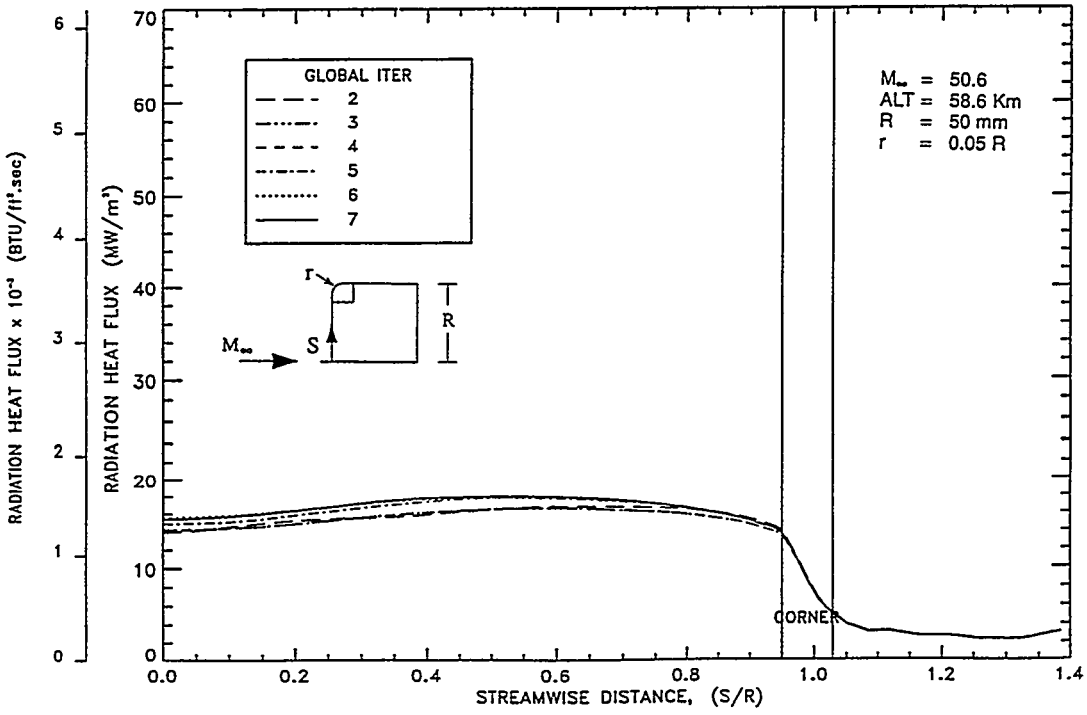

(c) Radiation heat flux convergence

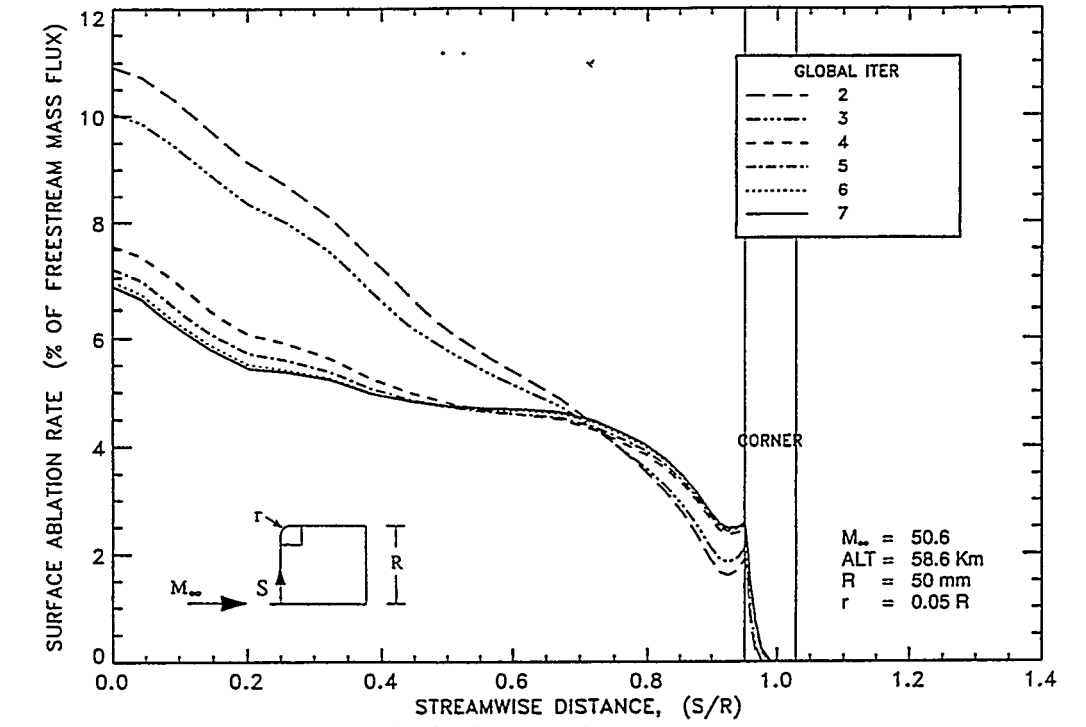

(d) Surface ablation convergence

Figure 3-14. LAURA - LORAN Global Convergence History or Variable Wall Temperature Test Case (Cont'd)

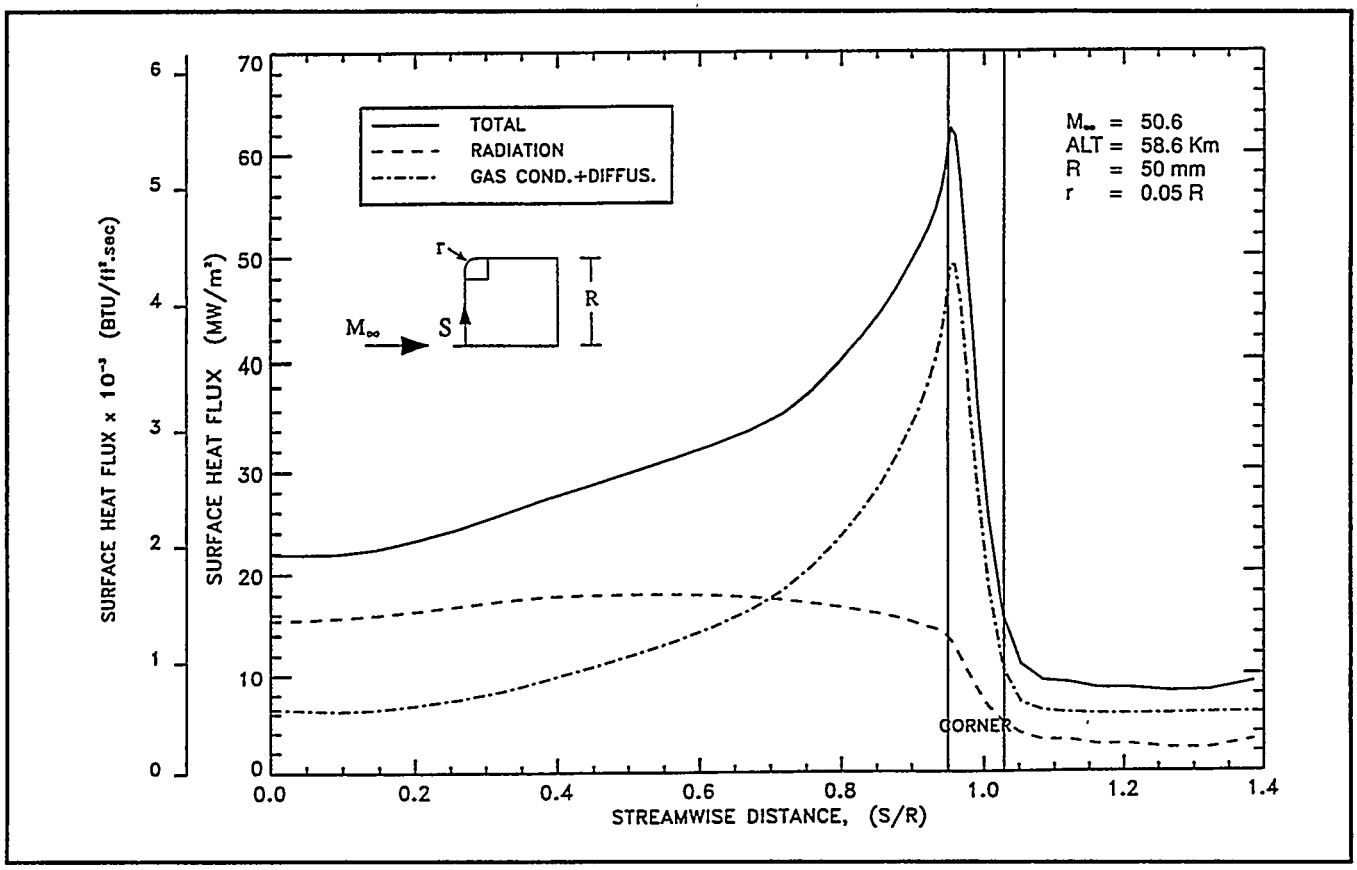

Figure 3-15. Heat Flux Components for Variable Wall Temperature Test Case

Global convergence has also been achieved for the constant wall temperature test case. As in the non-constant wall temperature case, a relaxation process to update the radiation field was found to accelerate convergence. The converged non-constant and constant wall temperature test case solutions are compared in Figure 3-16. The vertical line at S/R = 0.88 marks the location where the surface temperature distributions of the two test cases cross. Figure 3-16a shows that wall temperature, and the resulting thermochemical flowfield, have no effect on surface pressure. The total surface heat flux for the two cases is shown in Figure 3-16b. At the point of equal surface temperatures (S/R = 0.88) the total heat flux is nearly the same for the two cases showing that upstream effects are negligible. However, the surface ablation rate, shown if Figure 3-16c, reveals a 0.8% of freestream mass flux difference between the non-constant and constant wall temperature cases. This difference in ablation rate at S/R = 0.88, where the wall pressure and temperature are identical, is due to the differences is species mass fractions. The partial pressure of each species appears in the Knudsen-Langmuir relation used to compute surface ablation rates.

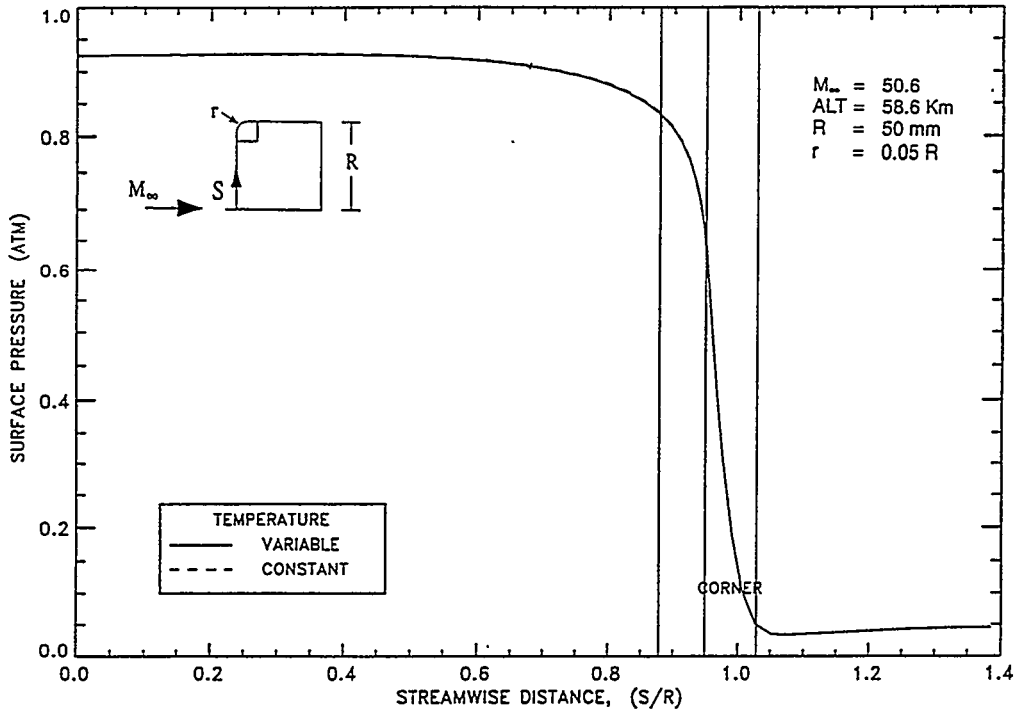

(a) Surface pressure

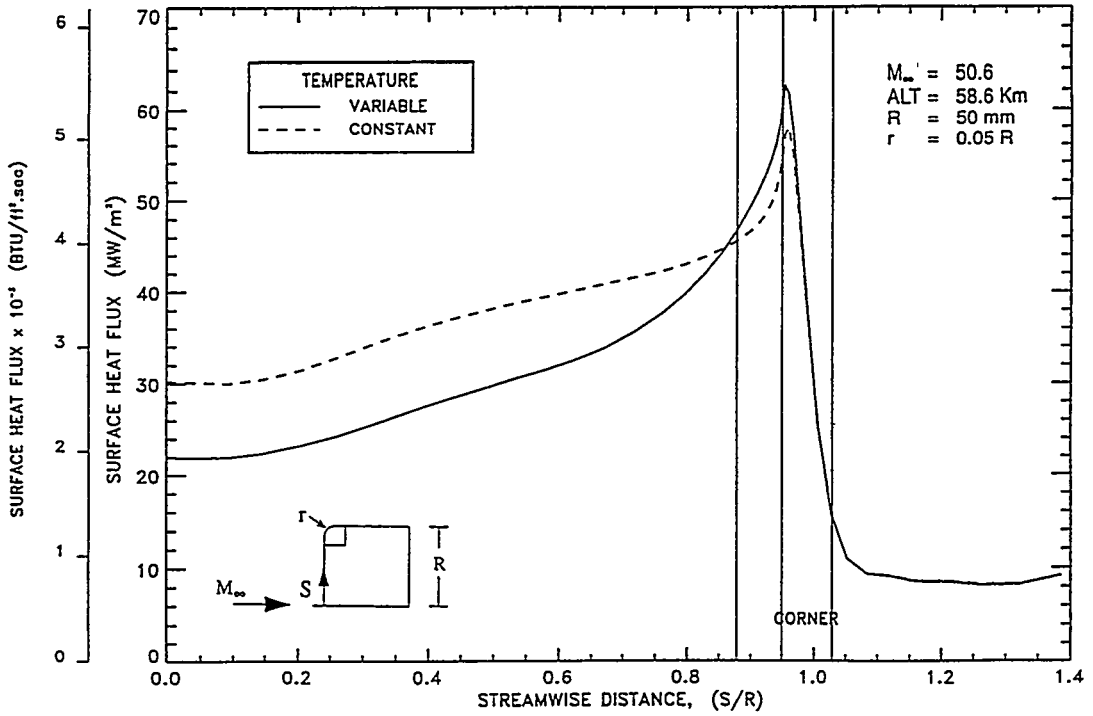

(b) Total surface heat flux

Figure 3-16. Comparison of Variable and Constant Wall Temperature Test Cases and the Effect of Upstream Influence

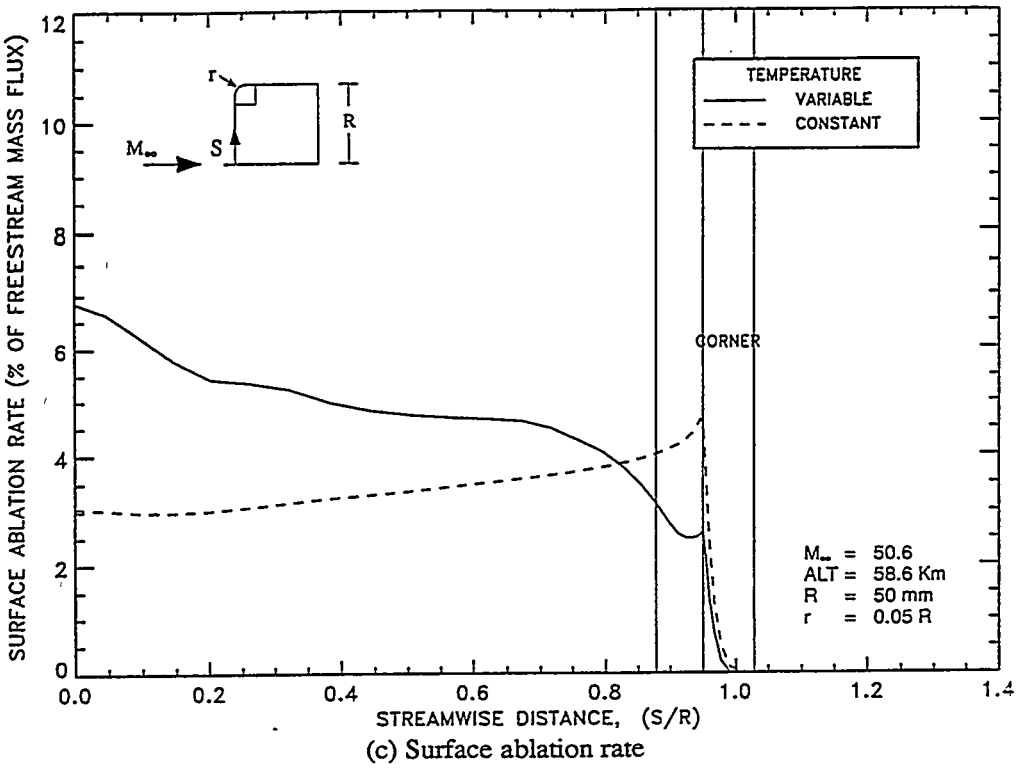

(c) Surface ablation rate

Figure 3-16. Comparison of Variable and Constant Wall Temperature Test Cases and the Effect of Upstream Influence (Cont'd)

A comparison of the two cases at the surface location, S/R = 0.88, where the surface temperatures were set to be identical is as follows:

1) Surface pressure for the two cases was identical;
2) The total surface heat flux, radiation plus convection, was nearly identical; and
3) The surface ablation rate for the constant wall temperature case is approximately 25% higher than that of the variable wall temperature case. This is equivalent to 0.8% of freestream mass flux.

Since the heat transfer rates are nearly identical between the two cases, the use of constant surface temperature would, with respect to ablation, produce conservative results near the front face edge, where surface temperature variation is high. Over the portion of the front face from the stagnation point outward to the edge, where the aeroshell is thinnest, the temperature variation is small, thus, approaching a constant wall temperature case. The ablation rate calculations of this portion of the front face area using a constant wall temperature would be higher, but very near those calculated with the non-constant temperature distribution. Therefore, performing CFD runs over a range of constant front face temperatures for selected trajectory points is the approach that will be taken.

On 11 May 1995, a meeting was held at the Building B facility in Valley Forge, Pennsylvania with APL and DOE personnel. At this meeting, presentations were made to provide an overview of: the reentry thermal work; plans for incorporating CFD results into SINRAP; and CFD results for test cases involving fixed and variable module front-face surface temperatures. A discussion was held on additional reentry work needed to be done and areas where APL personnel could support the Astro Space effort.

The first CFD trajectory point for the shallow case will be at the altitude of 273,219 feet which corresponds to six seconds from the time of module release. As discussed below, an approach was developed to determine heat transfer rates to be used in the SINRAP analysis, for the time duration up to the first CFD point.

Heat transfer by convection will provide the dominant influence on module temperatures for the transition flight regime as shock layer radiation at altitudes down to 273,219 feet will be relatively small. Convective heating results for the first CFD trajectory point will be used to determine the convective heat transfer coefficient to be used as SINRAP input at that specific time. At earlier times SINRAP input values will be based on calculated values from Reference 1, scaled by the ratio of the CFD value at six seconds divided by the calculated value from Reference 1 at six seconds. This approach provides a consistent method for coupling the convective heat transfer in the transition flight regime to that of the first CFD point. The SINRAP results for the first six seconds will then provide the starting point for incorporation of subsequent CFD output.

Reference

1. Cheng. H. K., "Hypersonic Shock Layer Theory of the Stagnation Region at Low Reynolds Number," Processing of the AGI Hat Transfer and Fluid Mechanics Institute (Stanford University Press), Stanford, CA, 1961, p. 161.

A preliminary SINRAP run was performed for the first six seconds of flight for the shallow trajectory. The results are preliminary for two reasons: (1) the CFD solutions used as input were not fully converged at the time the new SINRAP run was made, and (2) the CFD determined heat transfer values are to be a function of surface temperature. Thus, iteration is required until the SINRAP output temperature matches the temperature on which the input values of convection and radiation were based.

The convective heat transfer results from the CFD runs at altitude of 273,219 feet were used to determine the convective heat transfer coefficient to be used as SINRAP input at that time. Coefficients at higher altitudes during the first six seconds have been scaled to be

consistent with the six second value. CFD results at the six second point also showed that radiation was increased above previous analysis results due to non-equilibrium effects. Truncation theory for non-equilibrium radiation was used to calculate radiation at higher altitudes based on the CFD value at six seconds.

The preliminary SINRAP results are summarized in Table 3-2. The column labeled *Previous* is based on a past SINRAP run with equilibrium radiation and a convective coefficient which included use of β' curves. The column labeled *New* has convection and radiation input based on CFD results as described earlier. Note that the non-equilibrium radiation is small compared to the convective heat transfer but, as expected, higher than the previous value determined from equilibrium theory. In both cases the heat transfer due to ablation (term $\dot{m}\,\Delta h$) is calculated based on SINRAP output. The value of this term shows that the heat transfer due to ablation is negligible. Thus, nearly all of the heat going into the module at this point in trajectory is contributing to the module temperature increase. The preliminary SINRAP results show a new surface temperature at the stagnation point which is 200°F lower than the previous value. Also, the average front face recession after six seconds has been reduced from approximately 1.2 mils to 0.9 mils.

Table 3-2. Preliminary SINRAP Results from First Six Second Runs

Values at Six Second Point (273,219 Ft):

	Previous		*New*	
Q_{conv}	1014	($C_h\,\Delta h$)	790	(CFD)
Q_{rad}	20	(Equil.)	152	(Non-Equil., Prelim CFD)
$Q(\dot{m}\,\Delta h)$	4		3	
$Q_c + Q_r - Q_{\dot{m}}$	1030		939	
Surface Temperature at the Stagnation Point(°F)	5465		5275	
Average Front Face Recession (in)	.00117		.00086	

Q in Units of BTU/ft^2 Sec

The latest CBCF conductivity data from ORNL, including the results of action items from the 28 April 1995 meeting, have been incorporated into a version of SINRAP. The CBCF subroutines track nodal temperatures and time so that graphitization effects will be included in the heat-up phase once temperatures exceed 2273°K, as well as the cool-down phase from peak temperature. Anisotropic effects have been included to calculate the conductance for circumferentially or axially coupled nodes. Air infiltration effects will be

added once the ORNL argon data have been modeled. This additional test data is expected by the end of October 1995. Once testing of the new routine has been completed and sensitivity studies performed, the new subroutine will be incorporated into the production version of SINRAP.

Revision B of the SINRAP program which includes the most current algorithm for CBCF thermal conductivity was debugged. A draft PIR documenting the revisions was prepared. Verification runs for shallow and steep reentries under random tumbling and face-on-stable orientations for revision B were started.

Unconverged data from the CFD analysis for the first three trajectory points of the shallow reentry were input into a modified SINRAP program as a test case. This modified program is the precursor to Revision C of the SINRAP program which will update Revision B to include the option to use CFD heating, ablation, and enthalpy data in place of the existing analysis. The CFD data are input to SINRAP through nodal tables that are generated outside of SINRAP. The test case is using CFD convective heating, wall enthalpy, and ablation for a portion of the trajectory. Existing analytical models are being used for the rest of the trajectory and for the radiation terms. The portion of this SINRAP test run which incorporated uncoupled RACER output for the first three CFD trajectory points (nine cases since each trajectory point has three wall temperatures) was successfully completed. Since the CFD output did not include radiation for these cases, previously calculated equilibrium radiation values were used. The purpose of this run was twofold: 1) to exercise the conversion program which converts CFD nodal output into the appropriate values for SINRAP surface nodes, and 2) to check out the SINRAP interpolation scheme for altitudes and temperature. In this case the variables converted were convective heating, ablation, and wall enthalpy. The SINRAP results for the first ten seconds compared well with previous results, indicating that both the conversion code and SINRAP were working properly.

Lockheed Martin Astro Space attended the INSRP RESP Review at Aerospace Corporation on 10 August 1995. The thermal analysis agenda was as follows:

- Brief Review of the Reentry Thermal Effort Since June 1994
- Incorporation of ORNL CBCF Conductivity Data into SINRAP
- SINRAP Modifications for CFD Input
- Review of Study on Effects of Imposed Surface Temperature Gradients on CFD Solutions

The coupling between CFD results and SINRAP was covered in detail. The outcome of the study to examine the effects of imposed module surface temperature gradients on the CFD computed results was also discussed. At the conclusion of this discussion the panel understood the decision to use a constant front face surface temperature for each CFD case.

During the September 1995 time period converged CFD results for the six second point (alt. = 273,219 ft.) was achieved. Using this data, a SINRAP run was performed for the first six seconds of flight for the shallow trajectory. The final converged stagnation node temperature at six seconds was 4142°F. This compares to the pre-CFD value of 5465°F. The primary reason for the lower temperature using CFD results is that the convection is about six tenths of the previous value.

Output from converged CFD analyses for the first five trajectory points has also been used to obtain preliminary SINRAP results for the first eighteen seconds of the shallow trajectory. Preliminary results in the stagnation region indicate that combined radiative and convective fluxes are significantly less than those predicted by the previous analysis. At the same time, the calculated ablation rate is also significantly less. The net result at eighteen seconds, three seconds prior to the expected time of peak heating, is a total recession which is approximately one third of the previously calculated value. The predicted surface temperature at this time, however, has risen to the point where it exceeds the values selected for the CFD runs. This is a consequence of having a smaller percentage of the external fluxes being removed by ablation, therefore more heat is being conducted into the aeroshell to raise its temperature.

Work on the reentry structural analysis was initiated in August 1995. A report detailing the modeling of the aeroshell FWPF stress-strain properties was completed (Ref. PIR-U-1VC4-Cassini-103). The significant feature of this model is that it accounts for the highly non-linear anisotropic behavior of the material at elevated temperatures. ABAQUS, a non-linear finite element code, was selected as the tool to perform the structural analysis. Generation of the ABAQUS aeroshell model has been completed.

Two options were considered for the use of thermal analysis results as input to the structural model. The first was to use temperature output from the SINRAP runs. The second was to use calculated external heat fluxes from SINRAP, which would require that the structural model be converted to a transient thermal model. It was concluded that the most efficient and accurate method would be to use temperatures, calculated by SINRAP at various points in the trajectory. The XYZ coordinates of the SINRAP nodal centroids have been determined so that appropriate transformation from SINRAP nodes to ABAQUS nodes can be made.

Consequence and Risk

Significant progress has been made in the consequence and risk portion of the safety analysis during this six month reporting period. Draft Methods Documents for the four major portions of the analysis have been completed and distributed (reference CON #1212, 10 May 1995). These documents are:

- Methods Document for the Global Transport and Dispersion of Radioactive Particulate (GEOTRAP) Code Draft version PIR: U-17C3-C/C096, date 21 April 1995
- Methods Document for the High Altitude Dispersion (HIAD) Code Draft version PIR: U-17C3-C/C097, dated 28 April 1995
- Methods Document for the Site Specific Analysis of Transport and Dispersion of Radioactive Particles (SATRAP) Draft version PIR: U-17C3-C/C094, dated 21 April 1995
- Methods Document for the Radiological Consequence Analysis Draft version PIR: U-17C3-C/C095, dated 28 April 1995

Completion of these draft documents was a significant step in the analysis process. The technical detail contained within these documents served to answer many of the questions and concerns which are listed in the INSRP PSAR Comments report. As of the end of September, no comments from INSRP on these documents had been received.

For the SATRAP analysis, effort has been continuing on the KSC wind field analysis. A computer program for graphically displaying wind roses was completed to process data from wind stations to display wind field characteristics in terms of wind direction and wind speed. Results were presented in the meetings with the INSRP Meteorology subpanel on 16 May 1995 and with the MET subpanel chairperson on 19 September 1995. To study the wind correlation at several locations and to examine the typical characteristics of the flow field, a large number of time sequence plots were generated and compiled for selected days of October, within launch windows, from 1987 to 1991. Also, as a screening process, this exercise has helped determine input anomalies. Work on the computer program to interpolate wind station data to a system of grid points was completed. Outputs have shown satisfactory results with smooth flow fields and flexibility in grid parameter definitions.

Work on the binary database for the meteorological conditions at KSC was initiated. These binary files provide time-dependent information such as turbulence conditions measured in stability classes, and mixing height, and will be used as companion files with wind

components files. A program for conversion of stability class to Monin-Obukhov length and for estimate of roughness length of water surface was generated. This completion of this task is pending availability of appropriate roughness length of vegetation and other land features.

The existing land use and demographic data base for the Cape Canaveral region was reviewed and some errors in data conversion were corrected. With the newly acquired data for surface characteristics from HNUS, this data base is currently being updated with more detailed information for the evaluation of agricultural production.

The screening dose analysis for animal products, seafood, and drinking water pathways was completed. This analysis was employed to support the selection of pathways to be included in the dose model of SATRAP. For the first year exposure, the screening analysis indicates that urban resuspension is the dominant pathway with 77.3% of the total collective dose, followed by direct inhalation during cloud passage with 22.6%. Other remaining pathways contribute less than 1%. Note that this result applies to a set of assumptions which include equal distribution of source term to all people in the grid area (with the majority living in urban areas) and particle size set at 1 micron. These percentages are expected to change for subsequent years, with a larger contribution from the ingestion pathway, because the cloud passage dose applies only to the first year and resuspension decreases with time. The screening analysis was performed for four hypothetical source term cases: 100% release (290,000 Curies), 20 Curies, air concentration set at 1 micro-Curie/cubic meter, and ground concentration set at 1 micro-Curie/square meter.

During the September 1995 time period, a comparison of the results from the screening analysis with the results from a published model (Boone et al., ``Terrestrial Pathway of Radionuclides Particulates," Health Physics 41, pp. 735-747, 1981) was performed. In general, the level of food contamination predicted by the Boone model was much higher than the result from the screening analysis. Due to the multitude of inputs involved in the evaluation, the cause of this difference is still under investigation.

The KSC vicinity food production data were updated for the Radiological Consequence Analysis methods document. The write up of a new appendix describing the process used in the KSC site-specific dose screening analysis, with results from the calculation spreadsheet, was completed.

The implementation of the ingestion model from common food production was completed. For the KSC area, PARDOS can now compute the ingestion doses from consumption of two

specific crops, meat, milk, water and seafood which include fish and crustacean. Doses from consumption of locally grown garden vegetables is also considered in the analysis. Any contaminated foodstuff with excess of production over local consumption, is converted to potential exposure doses for people living outside of the grid area. In order for the evaluation of these common doses to be representative, various inputs from the data base of local agricultural production must be prepared. Considering that most of the population will be inside of shelters during nighttime launch conditions, a reduction factor was added to the inhalation and cloudshine doses in the screening analysis. Also, the fresh fish pathway analysis was updated to reflect additional data recently obtained from the Florida Game and Fresh Water Fish Commission.

For launch constraints, information obtained thus far indicates that structural response and ground level concentration from toxic plume are a few conditions considered. Since these conditions are evaluated with computer codes at the launch site, the translation into wind speed or wind direction constraints are not available at this time.

Safety Test Program

End-On Test

The first RTG end-on impact test was successfully completed on 13 April 1995 at the Sandia Rocket Sled Test facility. The test article, designated TA#1, consisted of approximately one-half of a converter housing containing nine simulated GPHS modules. The outboard end of the converter, which was impacted against concrete, included the outboard heat source support system and pressure dome. The intended nominal impact temperature (1090°C) and velocity (56 m/sec) were achieved within the allowable range. Post test examination of the heat source indicated no breach of the iridium clads and the average measured strain of the clads after impact was consistent with Orbital Sciences Corporation hydrocode predictions. The detailed post test findings were documented by LANL.

The second end-on impact test was conducted on 24 May 1995. The second test article, designated TA#2, was impacted against concrete at a velocity of 75 m/sec (at a nominal temperature of 1090°C). Post test examination revealed breaches in several of the clads containing fuel simulant. LANL is in the process of documenting all post test inspections and findings, including clad deformations, particle size distribution of the fuel simulant, etc.

Edge-On Fragment Test

An engineering test was conducted on 22 June 1995 at the Sandia Rocket Sled Test Facility to evaluate the effects of rigidly mounting a test fragment to the sled for the edge-on impact test. No converter or heat source hardware were involved in the test. A rigidly mounted aluminum fragment (.063 inch thick) was propelled into a 0.3 inch thick steel cylinder at ~1025 fps. The fragment did not "pull out" from its mounting during acceleration down the track, as occurred in a previous test, but it did deflect ~2 to 3 inches due to aerodynamic forces prior to impact. Little damage to the steel cylinder was reported but the test fragment appeared to shatter upon impact.

After evaluating the results of this test, it was decided to perform an additional engineering test. The test will be performed in the reverse sequence of the test described. For this test an aluminum cylindrical shell (representative of the converter housing) will be mounted on the rocket sled and impacted into a free standing aluminum fragment. The fragment material and size will be the same as in the 22 June test. The velocity of the cylindrical shell will be 1000 fps (nominal). Testing is planned in early October 1995. Meanwhile, the three converter test articles are being stored at Lockheed Martin Astro Space until the final test sequence and mounting requirements are determined.

Task 4

Qualified Unicouple Fabrication

TASK 4
QUALIFIED UNICOUPLE FABRICATION

The remaining efforts in Task 4 are associated with testing of 18 couple modules. Test temperatures and life test hours are shown in Table 4-1. All modules continued to show normal performance. The most significant events during this reporting period were:

18-11 – Reached the 10,000 hour test milestone on 20 April 1995
18-12 – Reached 1 year of operation on 21 August 1995

Table 4-1. Test Temperatures and Life Test Hours

Module	Unicouple Source	Test Temperature Hot Shoe	Status as of 1 October 1995
18-10	Early Qualification Lot	1135°C	10,400 hours Performance Normal Test Terminated October 1994
18-11	Full Qualification Lot	1135°C	13,936 Hours Performance Normal
18-12	Early Flight Production Lot	1035°C	9,760 Hours Performance Normal

18 Couple Module Testing

Two modules remain on life test. Testing of module 18-10 was terminated at the end of October 1994 after 10,400 hours.

Module 18-11 (1135°C)

On 1 October 1995 the module reached 13,936 hours at the accelerated hot shoe temperature of 1135°C. Measured performance during this period continues to fall within the data base established by MHW and GPHS 18 couple modules. The 10,000 hour milestone was reached on 20 April 1995.

The thermoelectric performance evaluation primarily studies the trends of the internal resistance and power factor. Figures 4-1 and 4-2 show these trends in comparison to module 18-8, the last module built during the GPHS program. Agreement is excellent and provides a high degree of confidence that the GPHS unicouple manufacturing processes have been successfully replicated. Table 4-2 summarizes the initial and 13,936-hour performance data.

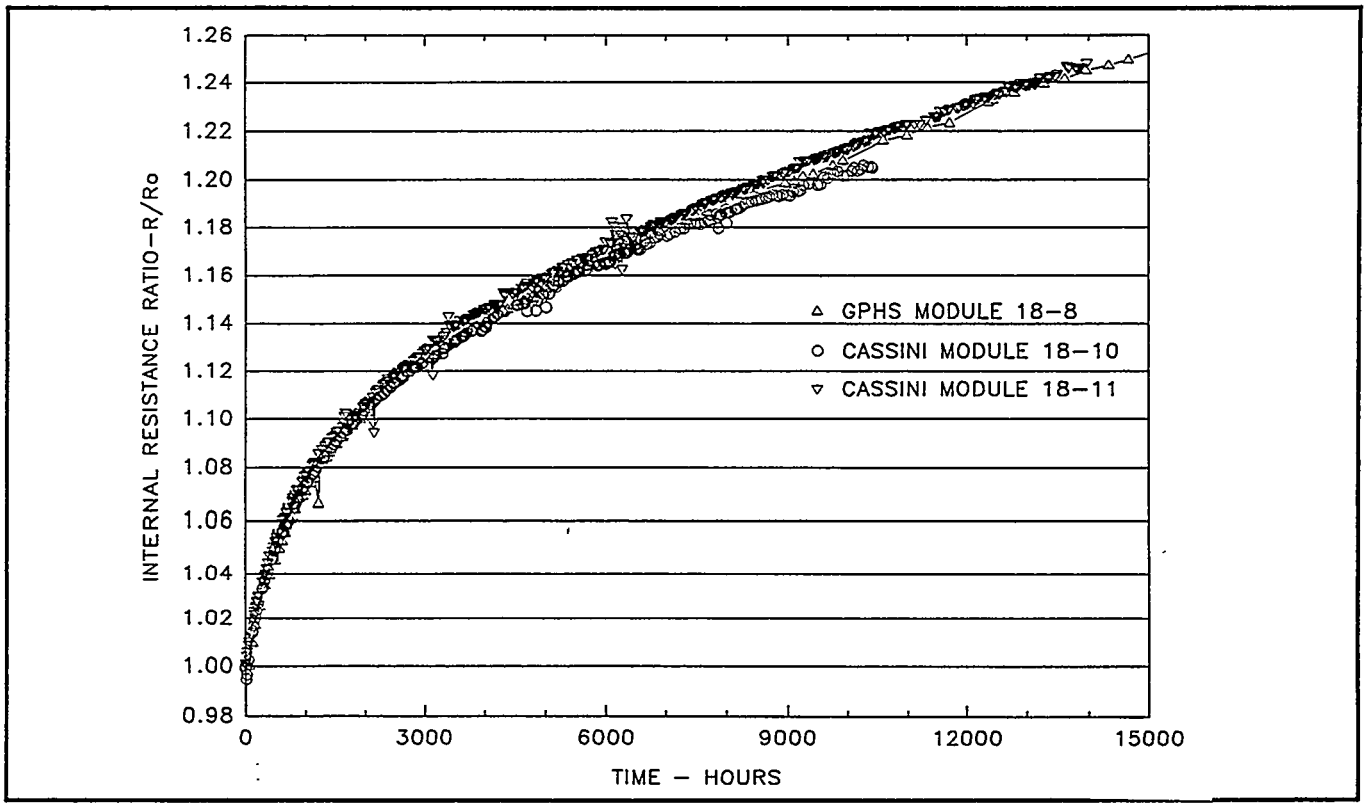

Figure 4-1. Internal Resistance Ratio Versus Time (Modules 18-10, 18-11, GPHS Module 18-8) – 1135°C Operation

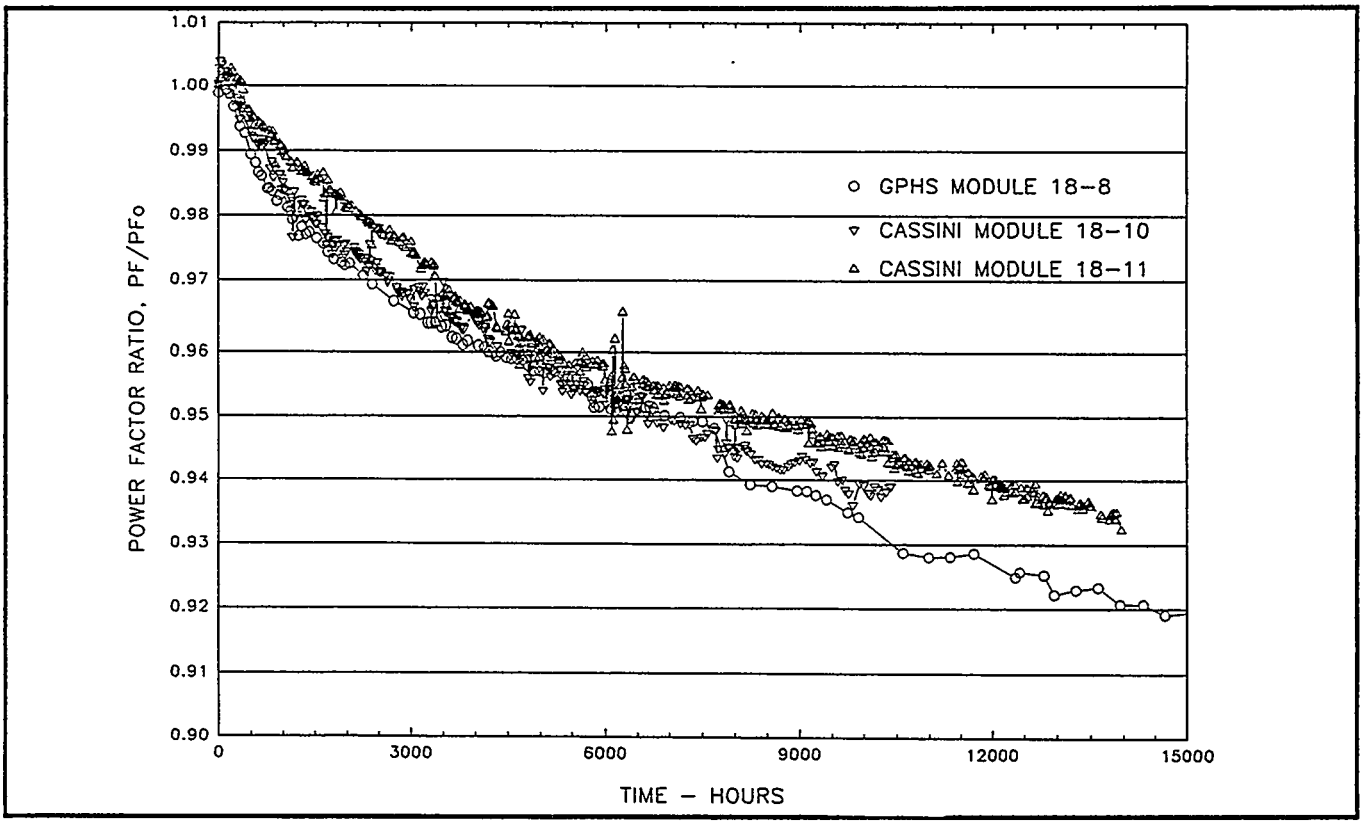

Figure 4-2. Power Factor Ratio Versus Time (Modules 18-10, 18-11, GPHS Module 18-8) – 1135°C Operation

Table 4-2. Comparison of Initial and 13,936 Hour Performance of Module 18-11 at 1135°C

	Initial 2/2/94	t = 52 hours V_L = 3.5V 2/4/94	t = 13,936 hours 10/1/95
Heat Input, Watts	190	192.9	193.4
Hot Shoe, °C Average	1137.8	1137.5	1114.3
Hot Shoe Range °C	5.4	5.2	7.8
Cold Strap, °C Average (8 T/Cs)	311.9	314.3	306.6
Cold Strap Range (8T/Cs)	2.6	2.5	2.4
Cold Strap Average (12 T/Cs)	306.5	308.9	301.5
Cold Strap Range (12 T/Cs)	20.1	20.3	19.1
Load Voltage, Volts	3.895	3.499	3.497
Link Voltage, Volts	0.108	0.121	0.099
Current, Amps	2.842	3.174	2.85
Open Circuit Voltage, Volts	7.140	7.160	7.522
Normalized Open Circuits (8T/Cs)	6.319	6.359	6.814
Normalized Open Circuits (12 T/Cs)	6.276	6.316	6.77
Average Couple Seebeck Coefficient (12)	498×10^{-6}	501×10^{-6}	537.3×10^{-6}
Internal Resistance, Ohms	1.104	1.115	1.378
Internal Resistance Per Couple (Avg.)	0.0613	0.0620	0.0765
Power Measured, Watts (Load + Link)	11.375	11.492	10.25
Power Normalized, Watts (8 T/Cs)	8.909	9.065	8.41
Power Normalized, Watts (12 T/Cs)	8.789	8.942	8.30
Power Factor	40.452×10^{-5}	40.557×10^{-5}	37.72×10^{-5}
Isolation			
Circuit to Foil, Volts	-1.68	-1.36	-1.60
Circuit to Foil, Ohms	6.29K	5.95K	0.8K

The isolation resistance trend between the thermoelectric circuit and the foil is shown in Figure 4-3 with modules from the MHW and GPHS programs. The isolation resistance plateaued at about 1000 ohms between 6,000 and 7,000 hours. It then started a slow decrease and is presently at 800 ohms. A similar plateau and gradual decline was observed in MHW module SN-1. At the accelerated temperature of 1135°C the same amount of sublimation occurs in about 1,650 hours of testing as would occur in a 16 year Cassini mission.

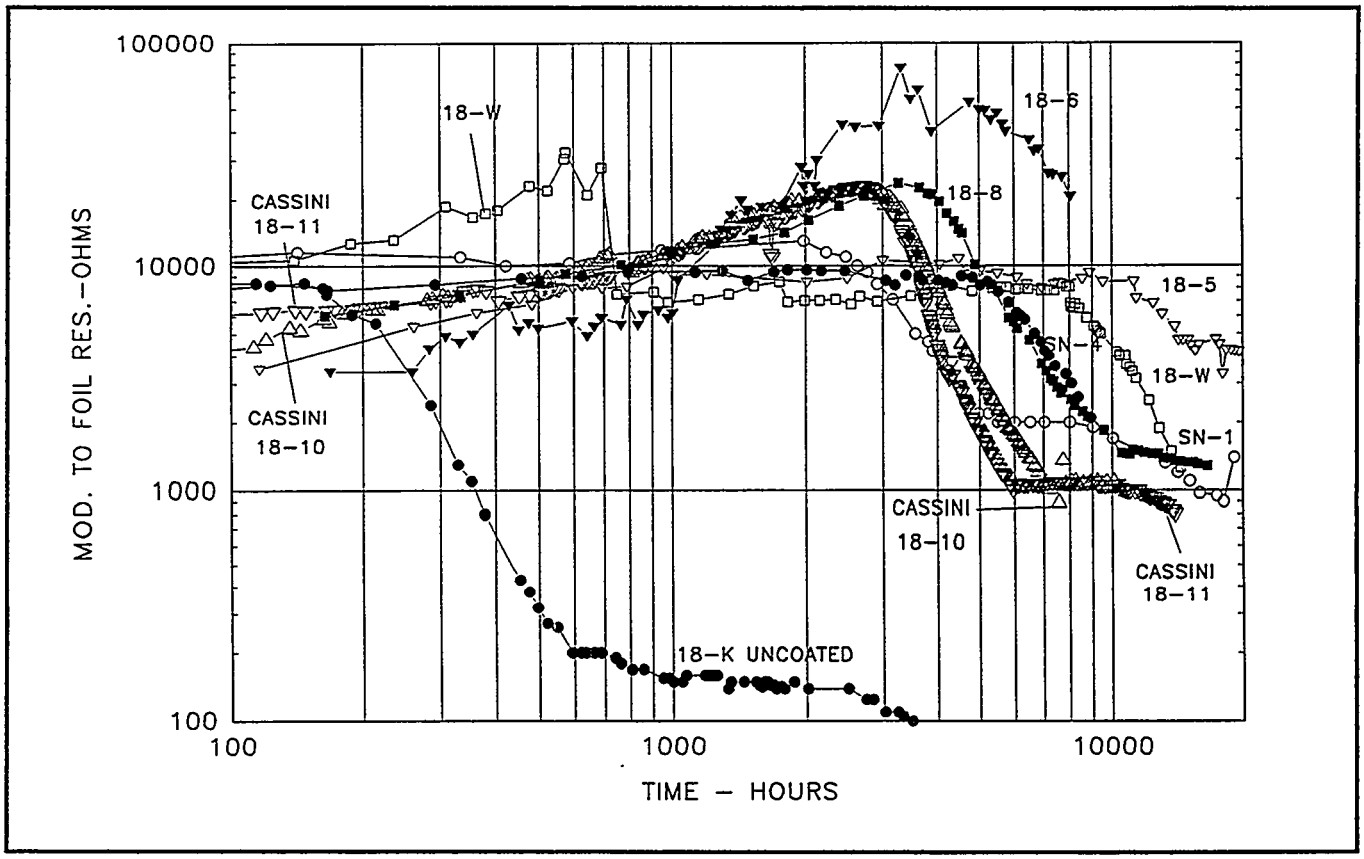

Figure 4-3. Isolation Resistance – Module Circuit to Foil (Modules 18-10, 18-11, GPHS Module 18-8) – 1135°C Operation

Consequently, approximately 8.4 times as much sublimation has occurred during the test duration of module 18-11 as will occur during the Cassini mission. The module performance, therefore, confirms the adequacy of the silicon nitride coating on the qualification couples.

Individual Unicouple Performance:

The performance of individual unicouples and rows of unicouples continue to be observed. Table 4-3 shows the room temperature resistance changes and the internal resistance changes observed during operation for each of the six rows and for individual unicouples in Rows 2 and 5. The unicouples continue to perform within a narrow band.

Table 4-3. Module 18-11 Internal Resistance Changes

Position	Serial #	2nd Bond Milliohm	Preassy Milliohm	Delta ri Milliohm	T = 0 Milliohm	T=1,509 Hours	Delta ri Milliohm	Percent Increase	T=13,936 Hours	Delta ri Milliohm	Percent Increase
1.0	H2006	22.50	22.10	-0.40							
2.0	H0507	22.40	21.90	-0.50							
3.0	H0512	22.7	22.20	-0.50	182.30	199.70	17.40	9.54	228.50	46.20	25.30
4.0	H0439	23.20	22.70	-0.50	62.30	67.90	5.60	8.99	77.40	15.10	24.20
5.0	H0587	22.50	22.40	-0.10	61.00	66.50	5.50	9.02	75.60	14.60	23.90
6.0	H0657	22.70	22.50	-0.20	61.40	67.30	5.90	9.61	76.90	15.50	25.20
					184.10	201.10	17.00	9.23	229.20	45.10	24.50
7.0	H0585	22.90	22.50	-0.40							
8.0	H0459	22.50	22.10	-0.40							
9.0	H0562	22.70	22.30	-0.40	185.70	203.20	17.50	9.42	232.70	47.00	25.30
10.0	H0248	22.70	22.30	-0.40							
11.0	H0163	22.90	22.40	-0.50							
12.0	H0282	22.70	22.40	-0.30	184.90	201.70	16.80	9.09	229.30	44.40	24.00
13.0	H0428	23.10	22.70	-0.40	62.10	67.90	5.80	9.34	77.40	15.30	24.60
14.0	H0326	22.60	22.00	-0.60	62.20	68.30	6.10	9.81	78.40	16.20	26.00
15.0	H0232	22.60	22.00	-0.60	60.90	66.60	5.70	9.36	76.30	15.40	25.30
					184.70	202.30	17.60	9.53	231.40	46.70	25.30
16.0	H0590	22.60	22.40	-0.20							
17.0	H0393	22.60	22.10	-0.50							
18.0	H0496	22.50	22.30	-0.20	184.20	201.40	17.20	9.34	229.00	44.80	24.30

Module 18-12 (1035°C Operation)

The module reached 9,760 hours at the normal operating temperature of 1035°C on 1 October 1995. Thermoelectric performance, as measured by internal resistance and power factor trends, continues to be normal as shown as Figures 4-4 and 4-5, respectively. Table 4-4 shows initial performance and the performance as of 1 October 1995

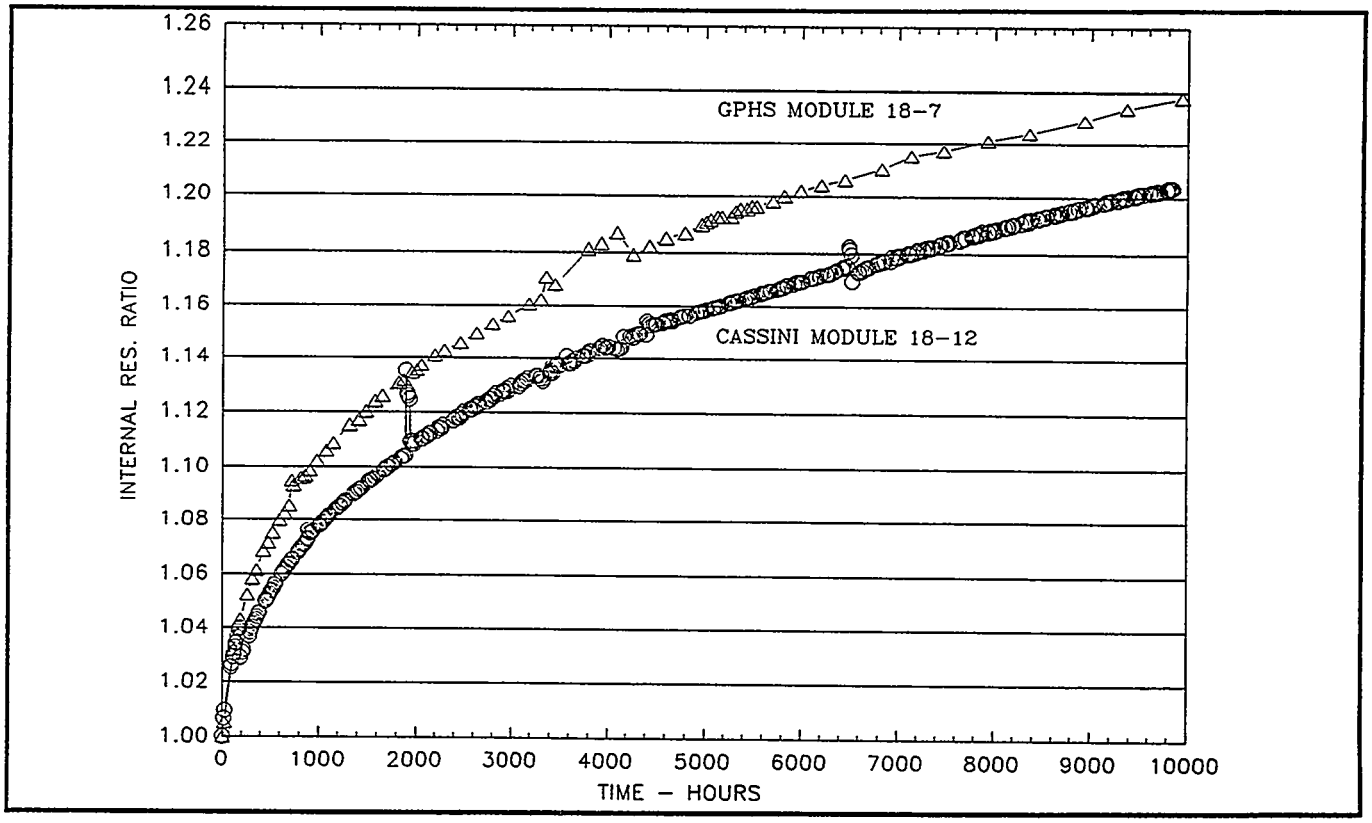

Figure 4-4. Internal Resistance Ratio Versus Time (Modules 18-12, and 18-7) – 1035°C Operation

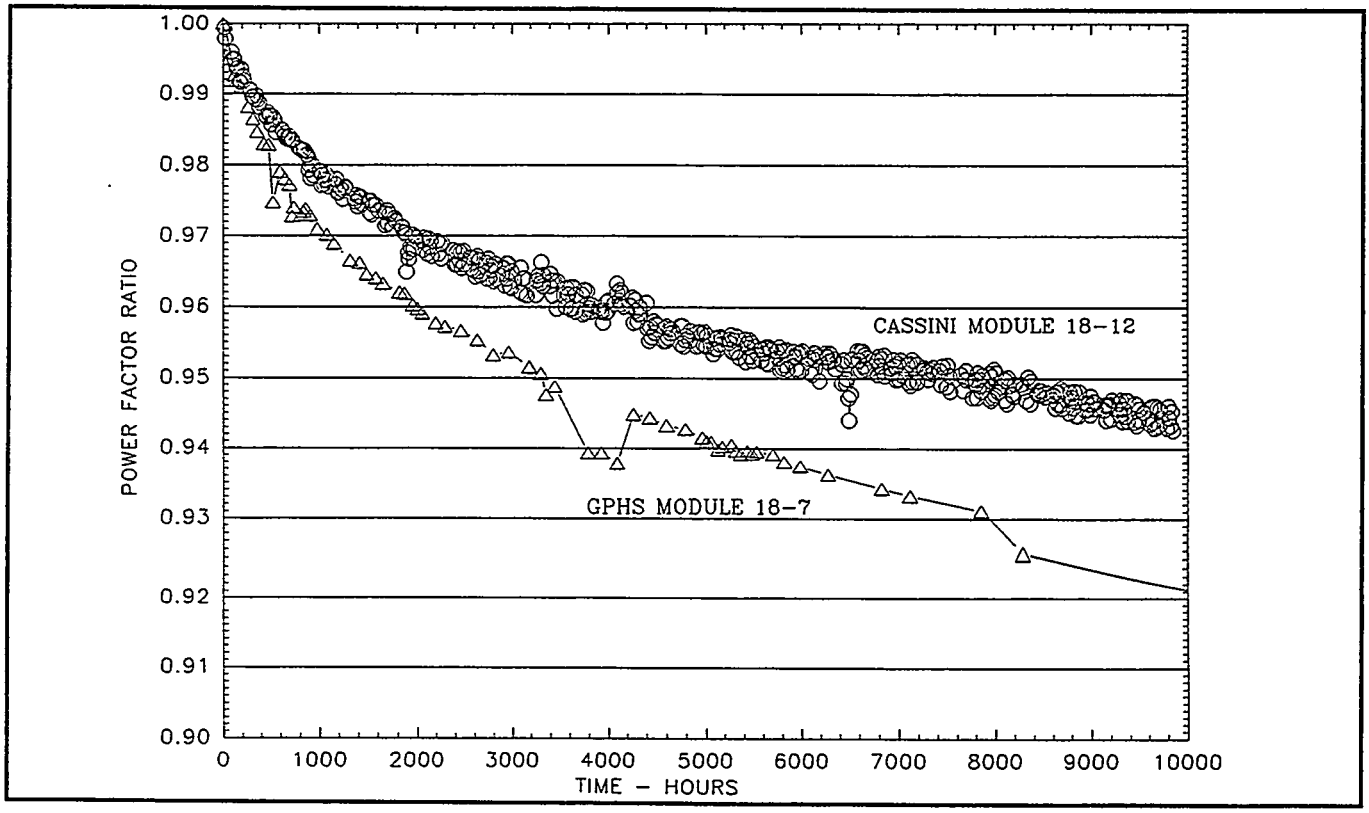

Figure 4-5. Power Factor Ratio Versus Time at Temperature (18-7 and 18-12) – 1035°C Operation

Table 4-4. Comparison of Initial and 9,760 Hour Performance of Module 18-12 at 1035°C

	Initial 6/16/94	t = 9,760 Hours 10/1/95
Heat Input, Watts	169.15	169.1
Hot Shoe, °C Average	1035.9	1029.0
Hot Shoe Range °C	5.7	4.5
Cold Strap, °C Average (8 T/Cs)	287.1	282.6
Cold Strap Range (8T/Cs)	5.0	5.1
Cold Strap Average (12 T/Cs)	282.7	278.2
Cold Strap Range (12 T/Cs)	19.8	19.5
Load Voltage, Volts	3.578	3.499
Link Voltage, Volts	0.155	0.155
Current, Amps	2.548	2.488
Open Circuit Voltage, Volts	6.431	6.824
Normalized Open Circuit (8T/Cs)	6.307	6.712
Normalized Open Circuit (12 T/Cs)	6.268	6.674
Average Couple Seebeck Coefficient (12)	497×10^{-6}	529.7×10^{-6}
Internal Resistance, Ohms	1.053	1.274
Internal Resistance Per Couple (Avg.)	0.0588	0.0708
Power Measured, Watts (Load + Link)	9.510	9.029
Power Normalized, Watts (8 T/Cs)	9.146	8.80
Power Normalized, Watts (12 T/Cs)	9.011	8.67
Power Factor	42.06×10^{-5}	39.64×10^{-5}
Isolation		
Circuit to Foil, Volts	-1.71	-0.864
Circuit to Foil, Ohms	21.3K	87.2K

Isolation Resistance

The isolation resistance between the circuit and foil continues to show the normal trend as shown in Figure 4-6.

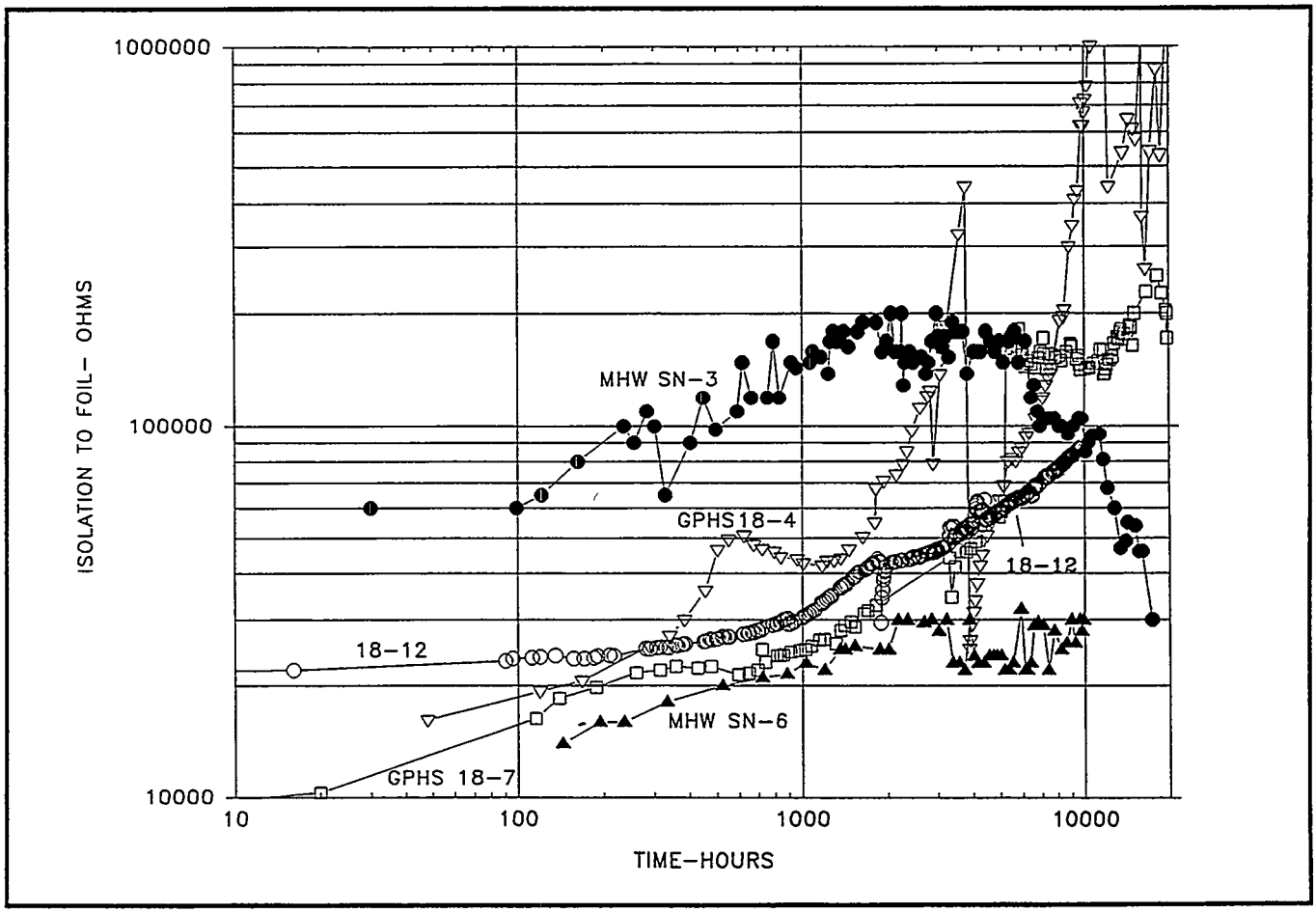

Figure 4-6. Isolation Resistance – Module Circuit to Foil (18-12, GPHS and MHW Modules) – 1035°C Operation

Individual Unicouple Performance

A review of the unicouple internal resistances and open circuit voltages indicates that all unicouples are exhibiting very similar behavior with time (See Table 4-5). The data for the six individually instrumented unicouples in Rows 2 and 5 are shown in Figure 4-7.

Table 4-5. Module 18-12 Internal Resistance Changes

Position	Serial #	2nd Bond Milliohm	Preassy Milliohm	Delta ri Milliohm	T = 0 Milliohm	T=1,505 Hours	Delta ri Milliohm	Percent Increase	T=9,.760 Hours	Delta ri Milliohm	Percent Increase
1.0	H2594	23.80	22.90	-0.90							
2.0	H2634	22.70	22.60	-0.10							
3.0	H2606	23.50	22.40	-1.10	176.80	192.10	15.30	8.65	210.50	33.70	19.10
4.0	H2168	22.20	21.70	-0.50	57.50	63.30	5.80	10.09	70.00	12.50	21.70
5.0	H2151	22.40	21.90	-0.50	57.40	62.90	5.50	9.58	69.20	11.80	20.60
6.0	H2256	22.20	21.70	-0.50	57.00	63.10	6.10	10.70	69.90	12.90	22.60
					171.20	188.60	17.40	10.16	208.40	37.20	21.70
7.0	H2597	24.40	23.20	-1.20							
8.0	H2680	22.60	23.00	0.40							
9.0	H2658	22.70	23.00	0.30	178.00	193.60	15.60	8.76	212.10	34.10	19.20
10.0	H1506	23.50	23.20	-0.30							
11.0	H1392	23.80	23.00	-0.80							
12.0	H1606	23.60	22.60	-1.00	176.20	193.40	17.20	9.76	212.70	36.50	20.70
13.0	H1344	23.60	23.50	-0.10	59.20	64.80	5.60	9.46	71.20	12.00	20.30
14.0	H1618	23.30	24.00	0.70	58.60	64.50	5.90	10.07	71.20	12.60	21.50
15.0	H1262	23.70	23.30	-0.40	59.40	65.00	5.60	9.43	71.40	12.00	20.20
					176.60	193.70	17.10	9.68	213.10	36.50	20.70
16.0	H1580	23.00	23.70	0.70							
17.0	H2127	22.80	22.10	-0.70							
18.0	H2113	22.90	22.20	-0.70	174.50	191.30	16.80	9.63	210.60	36.10	20.70

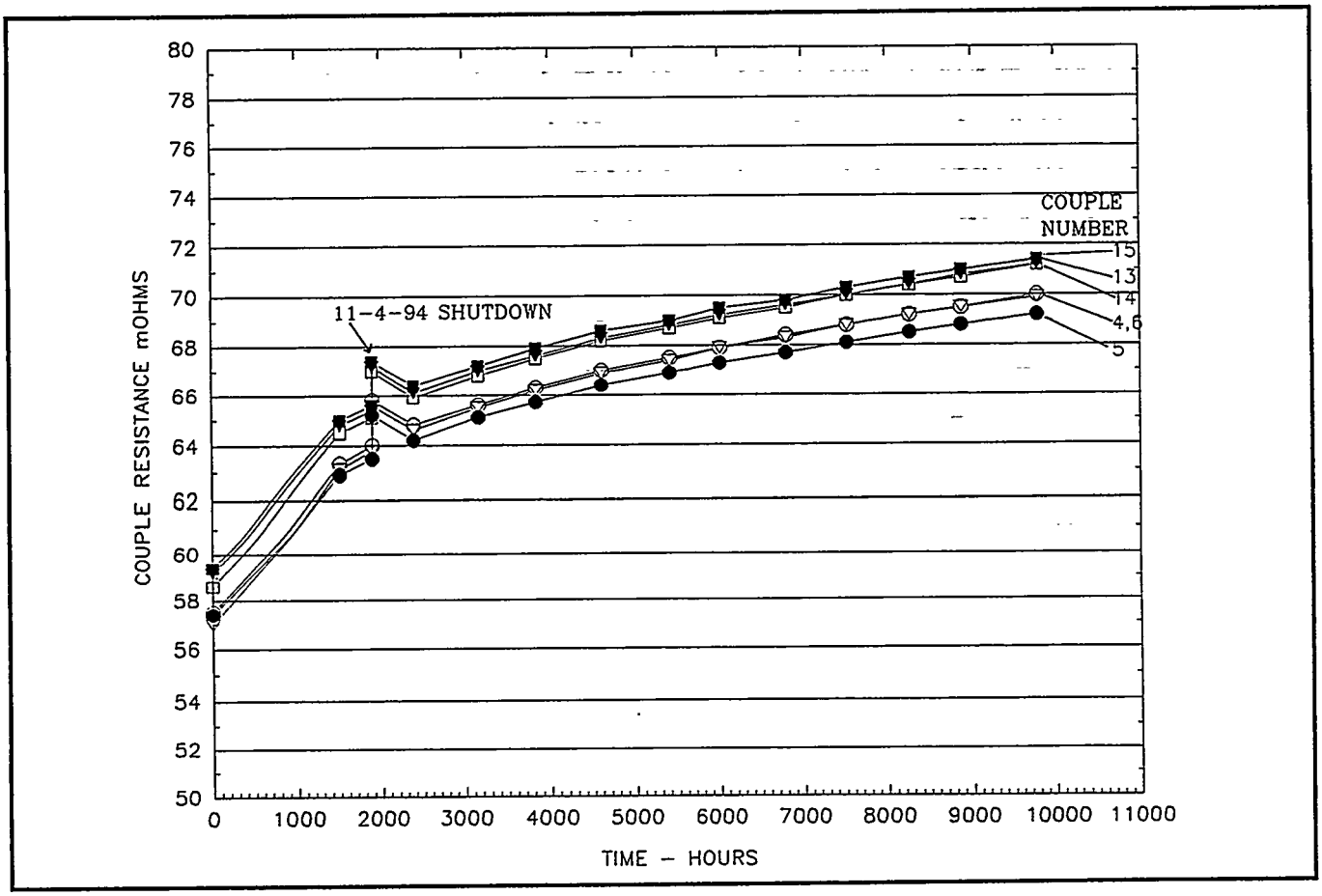

Figure 4-7. Individual Unicouple Internal Resistance Trends (Module 18-12)

Task 5

ETG Fabrication, Assembly, and Test

TASK 5
ETG FABRICATION, ASSEMBLY, AND TEST

E-6 ETG Test Activity (Building 800)

A Standing Instruction (SI) was prepared for storage of the E-6 ETG in Building 800. The SI defines the monitoring and re-pressurization procedures to ensure that proper argon gas pressure is maintained within the ETG and the converter shipping container (CSC) during the storage period. The ETG gas management valve (GMV) will remain open during storage so the ETG pressure can be read directly from the pressure gage mounted on the exterior of the CSC. Weekly monitoring of the ETG and CSC pressure continued during the storage period. The ETG has been re-pressurized three times to ensure its pressure is maintained at 1.5 psi (minimum) above the CSC pressure. The E-6 storage history is shown in Figure 5-1.

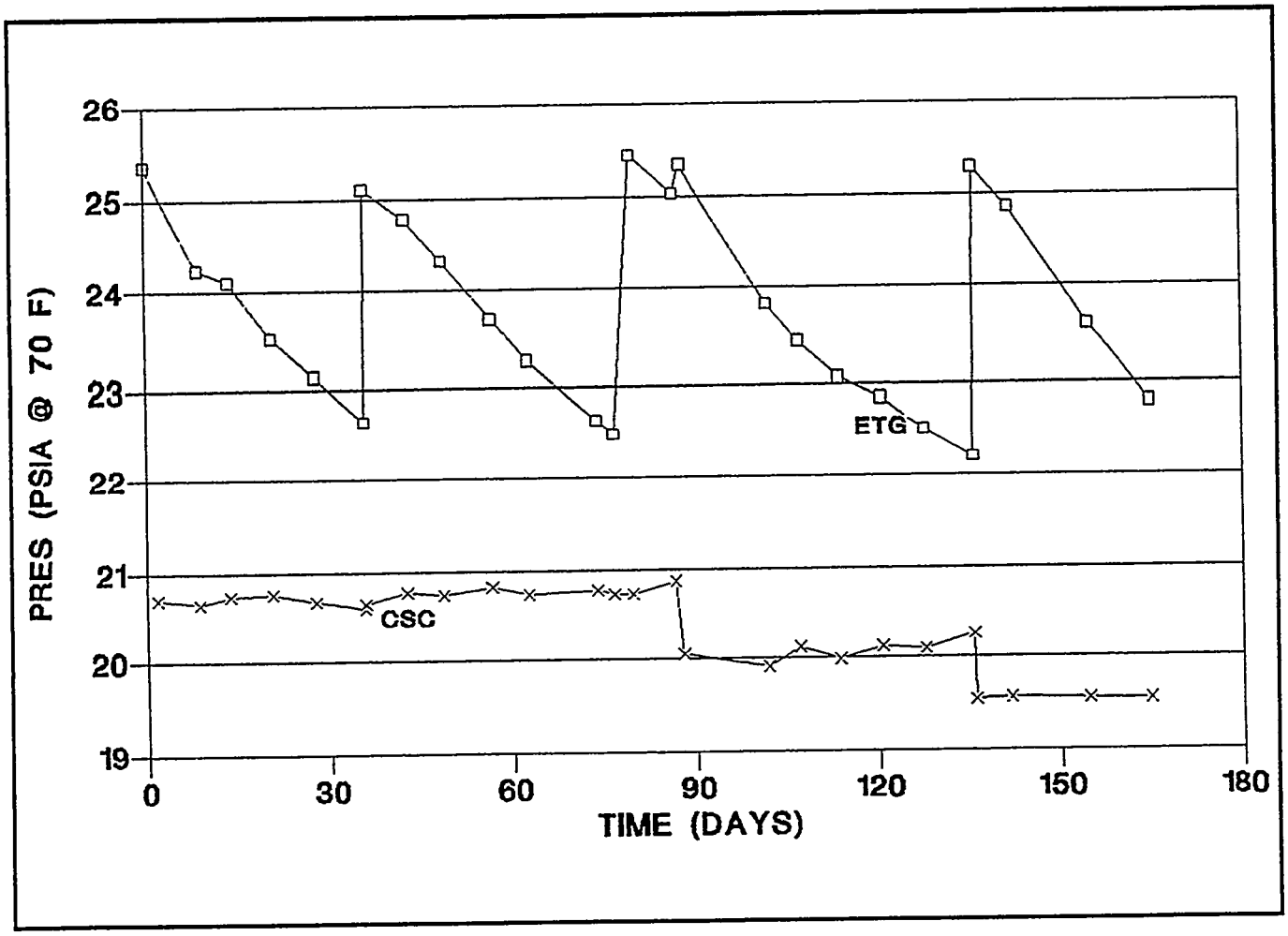

Figure 5-1. E-6 Storage History (ETG and CSC Pressures)

During July the ETG was pressurized by connecting the gas service cart to the converter shipping container. During this re-pressurization operation the filter in the CSC line was checked and replaced. Also, the GSE power cable connector was checked for proper pin retention force. It was determined that two pins required re-setting. This was accomplished in accordance with an approved test requirement (TR).

E-7 ETG

Inspection of the thermopile prior to insertion into the converter shell assembly was completed. The thermopile electrical resistance remained at 826 milliohms. Assembly of the inner moly frame support hardware was subsequently completed.

Insertion of the thermopile into the converter shell assembly and installation of the unicouple mounting screws and C-seals were completed the week of 1 May. Leak testing was successfully completed after removal and replacement of eight unicouple sealing screw seals. Pressure decay testing was started but three unicouple seals were found to be leaking and two small leaks were discovered at the gas management valve on the outboard dome. The unicouple seals and processing dome were replaced and the pressure decay test was repeated with acceptable results.

Assembly of the EHS into the converter was completed the week of 5 June. All electrical circuit and shunt resistances were verified to be within specification limits. Preloading of the heat source supports and midspan supports were completed and lock nuts and midspan caps were installed. The spool piece was installed and the EHS thermocouples and power cables were connected.

The inboard dome, the RTD cable assembly, and PRD adapter plate were installed on the ETG. A pressure decay test was performed and the requirements were met with a decay rate of 0.1 psi drop in 24 hours. A fit check of the PRD was successfully performed. This completed the ETG assembly.

The E-7 ETG was installed in the converter shipping container and delivered to Building 800 on 5 July. The E-7 ETG was installed into the LAS and a test readiness review was completed on 26 July. EHS heating was initiated after all vacuum requirements for the LAS and ETG were satisfied. On 31 July, it was observed that the ETG voltage and current output were less than other ETGs at the equivalent heat input.

Systems Test met with Engineering and Quality Assurance on 1 August to review the ETG performance data and to outline a course of action. Based on an engineering analysis, it was determined that a shunt between the negative and positive leads of the ETG electrical circuit could cause a low ETG voltage output. To address this issue the following actions were implemented:

1. The ETG power cable between the LAS and ROC was disconnected at the LAS. The ETG voltage was then measured at the LAS connector and found to be 1.8 volts compared to an expected voltage of approximately 3 volts. This measurement verified the cause was inboard of the LAS.

2. The ETG was then cooled to room temperature and the LAS was backfilled with argon gas. This permitted disconnecting the internal LAS cable and shorting module from the ETG power circuit. This confirmed that the problem was most likely within the ETG.

3. After reviewing the thermopile assembly procedures and specifically, the unicouple insertion map, it was seen that 144 unicouples were inserted with incorrect polarity. An error in the plotting software which generated the map was the cause of the problem.

Three options for correcting the problem were considered and evaluated. The options were:

1. Rework the E-7 thermopile by repositioning the reversed polarity unicouples.
2. Rework the E-7 thermopile by replacing the reversed polarity unicouples with E-8 unicouples.
3. Remove the E-7 thermopile and replace it with the E-8 thermopile, which is yet to be completed.

These three options and their trade-offs were reviewed with DOE on 7 August in order to finalize the recovery plan. DOE provided direction to proceed with Option 2 and a Rework Plan (Ref. CON #1300) and Corrective Action Plan (Ref. CON #1306) were issued.

On 7 August, the ETG was prepared for removal from the LAS by installing the outboard dome and midspan caps. The ETG was pressurized with argon gas and a pressure decay test was performed to verify sealing integrity. The ETG was removed from the LAS, electrical measurements were made, and the ETG was installed into the Converter Shipping Container (CSC). The ETG/CSC was moved to Building B on 10 August in preparation for disassembly and rework.

The detailed rework planning packages were initiated on an expedited basis. The first planning package to remove the ETG from the shipping container and install it on the assembly fixturing was initiated on 14 August.

Removal of the thermopile from the shell assembly was completed the week of 21 August. Rivet removal from the misoriented unicouples was begun the week of 28 August. All misoriented unicouples were removed and replaced by the end of September. The next planning package for unicouple forming and riveting was issued and the work is underway. Rework of the C-seal surfaces on the shell and fin assembly and oxidation of the balance of nut plates required for E-7 re-assembly were initiated during this reporting period. The rework schedule for E-7 is shown in Figure 5-2. At the end of this reporting period the rework activities are approximately six weeks ahead of schedule.

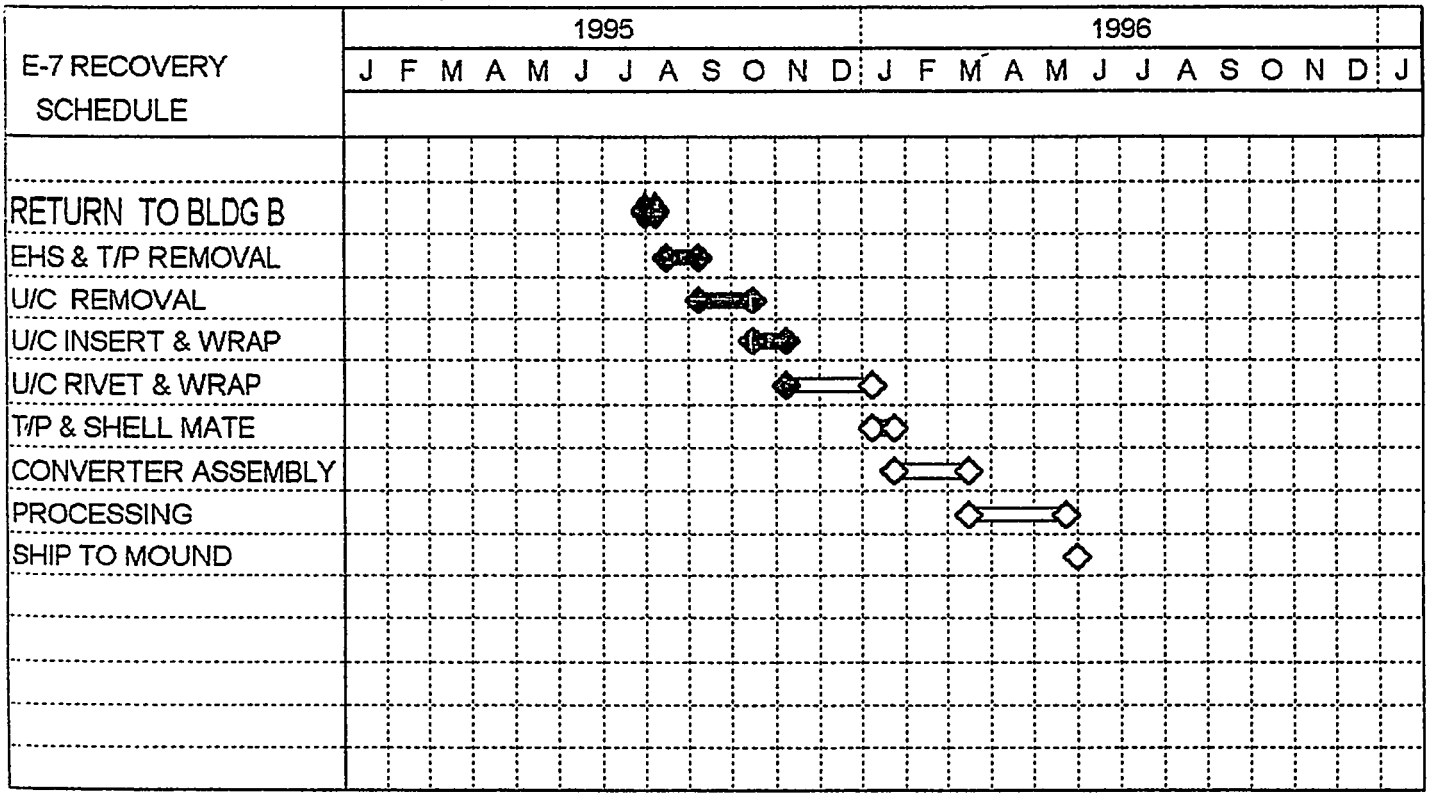

Figure 5-2. E-7 Recovery Schedule

E-8 Converter Hardware

Fabrication of subassemblies for the E-8 hardware kits continued during this reporting period. Several major components have been completed including the foil insulation package, nickel plated thermopile straps, and the gas management valve assembly. All hardware kits have been placed in stock and any shortages are being filled as the hardware completes the fabrication process.

A protective handling device has been designed and fabricated to provide rigid protection for the foil insulation package in the current configuration.

Final closure welding of the shell and fin assembly was completed. The assembly successfully passed the proof pressure and pressure drop tests. Preparations are underway to prepare the unit for the PD224 painting and curing process.

RTD Cable Assemblies

Fabrication of the E-7 and F-5 RTD cable assemblies was completed during this reporting period. Acceptance and protoflight testing were successfully completed on the F-5 RTD cable assembly, thereby qualifying the new RTD cable design. The F-5 RTD cable was shipped to Mound Laboratories on 30 August for F-5 RTG testing.

Fabrication of the E-2 and E-8 RTD cable assemblies is continuing. Nickel shield wrapping and potting of both connector and RTD headers were completed. Final air curing of the potting at elevated temperature was delayed due to furnace problems. Final curing is expected to be completed during the next reporting period.

Key Sourcing Items

The last lots of tungsten cold shoes used for spare unicouple production were accepted through Receiving Inspection during April.

Efforts to place a subcontract with GE-Nuclear to support safety analyses were discontinued during this reporting period because GE-Nuclear would not accept proposed terms and conditions of the purchase order. Sandia Laboratories is now under subcontract to perform this task.

Lockheed Martin Astro Space continued to work closely with Engelhard Corporation on the fabrication of iridium midspan can assemblies. Micro cracking was encountered in the legs after forming; however, the problem has been resolved and a total of nine can assemblies were successfully fabricated. These assemblies will be assembled into the E-8 and spare kits.

Task 6

Ground Support Equipment (GSE)

TASK 6
GROUND SUPPORT EQUIPMENT (GSE)

RTG Shipping Containers

Three shipping bases and cages were received from Mound for upgrading to the latest engineering requirements. The units were inspected, defects noted and dispositioned to rework to the drawing. The rework will be performed as materials are available since several items will have to be purchased for the rework.

Shipping cage modifications were initiated during this reporting period with the fabrication of the top hat section and the modifications to the existing cages to accept the top hat section. Modification of two of the cages will be completed in the fourth quarter 1995 and the balance in the first quarter 1996.

The E-6 and E-7 shipping container bases were reworked to incorporate an ECN to install a longer length guide pin to facilitate cage installation. Machining of the three converter support rings was completed. Machining of the smaller piece parts is continuing. The final assemblies will be completed in the fourth quarter 1995.

Read Out Console (ROC)

Two ROCs have now received Certificates of Inspection (C of I). During this reporting period two of the ROCs completed acceptance testing. Air blowers were installed in the ROC enclosures to provide additional air flow which is expected to reduce the instability of the ROC power supplies at maximum power levels. This instability was a continuing problem while processing the E-6 ETG.

Gas Service Cart (GSC)

One of the gas carts developed a small leak when attempting to perform a pressure decay test on E-7 during ETG assembly. The leak was traced to a cracked weld at a valve/tubing interface joint. The GSC was repaired by re-welding followed by leak checking and gas flow cleaning.

Task 7

RTG Shipping and Launch Support

TASK 7
RTG SHIPPING AND LAUNCH SUPPORT

RTG Shipping

The plans and procedures for the 18 inch drop test for the new RTG transportation system were reviewed and comments were provided to Westinghouse-Hanford. Follow-up phone conversations resolved open issues and the test was conducted at Hanford in June 1995. Lockheed Martin Astro Space supported the test with an on-site observer. The shock test loads were less than the pre-established limits and the test was successfully concluded.

A Lockheed Martin Astro Space representative attended a two-day meeting to review the progress on trailer fabrication and to review loading and unloading plans for the new transportation system. The first day of the meeting was held at the trailer fabrication plant (Mobilized Systems, Inc., Cincinnati, Ohio) and the second day at the Mound plant.

Discussions were held with JPL on the options and methods to be used at the Kennedy Space Center (KSC) for loading and unloading the new RTG transportation system. Primary attention is being directed toward the interfacing of site equipment and facilities with the new transportation system. Contingency situations and possible back-ups were evaluated for alternate power and cooling for the containment vessels. It was determined that the new facility transporter will not be used to move RTGs once they arrive at KSC. Instead, a fork lift will be used to unload and load the van and move the RTGs between the vans and storage building. This method is consistent with the methods used for the Galileo and Ulysses RTGs.

Task 8

Designs, Reviews, and Mission Applications

TASK 8
DESIGNS, REVIEWS, AND MISSION APPLICATIONS

8.1 Galileo/Ulysses Flight Performance Analysis

No significant activity this reporting period

8.2 Individual and Module Multicouple Testing

This task was successfully completed last reporting period and the results reported under Task 8.5.

8.3 Structural Characterization of Candidate Improved N- and P-Type SiGe Thermoelectric Materials

This task has been successfully completed.

8.4 Technical Conference Support

Internal and DOE reviews and approvals were completed for papers which were presented at the IECEC held in Orlando, FL, during the first week in August 1995.

- "Cassini/RTGs Small Scale Module Tests - Part Two" by C. Edward Kelly and Paul M. Klee.
- "Evaluation of an 18 Couple Module Composed of Improved Performance SiGe Unicouples" by C. Edward Kelly, Paul M. Klee, and Robert F. Hartman.
- "Radioisotope Thermophotovoltaic Generator for Space Power Applications" by Dr. S. Loughin and Dr. P. Uppal.

Mr. P. Klee and Dr. S. Loughin presented the papers.

8.5 Evaluation of an Improved Performance Unicouple *Module 18-Z*

This task has been successfully completed.

8.6 Solid Rivet Feasibility Study

This task has been successfully completed.

8.7 Computational Fluid Dynamics (CFD)

Work continues on the CFD task with a projected completion of October 1995. Because this task is closely related to the Task 3 safety activities, its technical progress is reported under that task.

8.8 Technical International Conference Support

This task was completed with the attendance by Mr. J. Braun at the ICT 95 Conference in St. Petersburg, Russia, in late June 1995.

8.9 Additional Safety Tasks

Additional safety tasks in the areas of uncertainty analysis, RTG case failure, and meteorological effects on safety for a November launch were added and are being implemented.. Because these efforts are closely related to the Task 3 safety activities, technical progress is being reported under that task.

Task 9

Project Management, Quality Assurance and Reliability, Contract Changes, Non-Capital CAGO Acquisition, and CAGO Maintenance

TASK 9
PROJECT MANAGEMENT, QUALITY ASSURANCE, AND RELIABILITY

9.1 Project Management

Task 9.1 Project Management

All weekly and monthly contractual reports were delivered on schedule.

The E-6 pre-ship review was held at Valley Forge on 6 April 1995. A number of documentation issues arose which were eventually settled and a DD250 was signed by DOE, signifying its receipt by the Government. Direction was received to hold E-6 at Valley Forge under bonded storage until it is needed at Mound.

During processing of the E-7 ETG it was observed that the ETG voltage was less than other ETGs at the equivalent heat input. A review of the problem was held at DOE in Germantown, MD. The problem was the result of 144 unicouples whose polarity was reversed due to a software error in the printing routine of the unicouple map drawing. A recovery plan was presented to DOE and approved. The target ship date of E-7 to Mound is 30 May 1996.

Attached are the Cassini RTG program calendars for 2Q95 and 3Q95 showing program meetings and important related events.

No significant environmental, health, or safety incidents occurred during this period.

9.2 Quality Assurance

Quality Plans and Documents

No plans were initiated or modified during this period.

Process Readiness and Production Readiness Reviews

No process or production readiness reviews were conducted during this period. A test readiness review was conducted prior to the start of processing of the E-7 converter.

Quality Control in Support of Fabrication

Assembly of the E-7 converter proceeded with few problems and was completed in June. It was transported to Building 800 where it was prepared for processing and acceptance testing. Early in the processing of the converter it was noted that the output from the thermoelectrics was lower than previous converters. Investigation of the converter fabrication history revealed that 144 unicouples were installed with incorrect polarity. The converter is now being reworked to correct this condition. The rework effort is proceeding well and no significant quality problems have been noted.

Work on sub-assemblies for E-8 is continuing, but at a lower priority in order to support rework of E-7. No significant problems have been noted for the E-8 hardware.

RTD Failure Review Board Activity: The FRB Failure Review Board continued to investigate the failure noted during qualification testing of the RTD cable assembly. It was suspected that the problem was in the RTD sensors, as purchased from Rosemount. When the cable assembly was separated from the sensor, the low isolation resistance remained on the sensor side while the remaining assembly demonstrated high isolation resistance. A sensor was sent to Rosemount for evaluation and it was concluded that the problem was caused by moisture trapped within the hermetically sealed sensor during fabrication. All of the sensors in house were tested; four were returned to Rosemount to be reworked and the balance were acceptable.

The Failure Review Board activity was concluded and a final report was issued. Also, a separate qualification report was issued by Engineering which qualified the RTD cable design. Based on these findings, the open non-conformance report was closed and the RTD design was accepted.

Unicouple Production

Unicouple production was completed in April. Some problems were noted in several processes during April, but, since production was ending, no immediate corrective action was taken. An effort is underway to update specifications and drawings, where necessary, to provide guidance for use in future production efforts. All unicouple fabrication processes were documented on video tape in accordance with DOE direction.

Quality Assurance Audits

Audits in the unicouple area have been discontinued since production has been completed. Audits were performed in the converter manufacturing area and on software configuration control. No significant problems were noted.

Quality Assurance Status Meeting

No status meetings were held during this reporting period.

Task H

Contract Acquired Government-Owned Property (CAGO) Acquisition

TASK H

CONTRACTOR ACQUIRED GOVERNMENT OWNED (CAGO) PROPERTY ACQUISITION

Task H.1 CAGO Unicouple Equipment

No significant activity during this reporting period.

H.2 CAGO - ETG Equipment

No significant activity during this reporting period.

H.3 CAGO - MIS

No significant activity during this reporting period.

H.4 CAGO (Building 800)

Refurbishment Items for Building 800

During the processing of E-6, it was noted that some facility items required rework. It was planned to refurbish the following prior to processing the E-7 ETG:

- Install new bellows type valves, new solenoid valve, tubulation, and a 60μ filter into the argon gas backfill system.
- Re-work cryopump compressor to eliminate oil and helium leakage paths.
- Install a deflector on inside of LAS to direct gas flow during backfills.

During April and May the installation of the new argon backfill system was completed, cleaned, and leak checked.

After conferring with the cryopump compressor manufacturer it was determined that the compressor would require replacement. The new unit was purchased from CTI and was installed prior to processing E-7.

The deflector on the inside of the LAS was also installed prior to processing E-7.

Program Calendars

Cassini Calendar

As of 27 September 1995

3rd QTR 1995

	M	T	W	T	F	S	S	FW
JULY	3 HOLIDAY	4 HOLIDAY	5	6	7	8	9	27
	10	11	12	13	14	15	16	28
	17	18	19 Quarterly Program Review - OSC Germantown, MD - Hemler, et al	20	21	22	23	29
	24 Monthly Reports Due to DOE	25	26 LASEP-T SPARRC Integration - San Jose, CA- *Braun/Rosko/Loughin* Decon Cover Fabrication Review - LANL, Albuquerque, NM - *Retnstrom*	27	28	29	30	30
AUGUST	31	1 IECEC - Orlando, FL - *Hemler/Loughtn/Klee* RTG Transportation System Review - Cincinnati/Mound, Ohio - *Cockfield*	2	3	4	5	6	31
	7 E-7 ETG Meeting w/DOE - Germantown, MD - Hemler, Hartman, Haley, Kugler	8 LASEP-T/SPARRC Uncertainty & Integrqtion - San Jose, CA - *Rosko/Loughtn/Kampas/ Braun*	9	10 RTG Installation Cart Review - JPL, CA - *Haley* PSSP RESP - Aerospace, Los Angeles CA - *Braun/Dayuttt/Tobery, et al*	11	12	13	32
	14	15	16	17	18	19	20	33
	21	22 F-5 Magnetics Walkthrough - EG&G Mound - *Cockfield*	23 INSRP LASP PSAR Comment Review - Valley Forge - *Braun, et al*	24 Monthly Reports Due to DOE INSRP Review Launch Accident/ Uncertainty - Valley Forge - *Braun, et al*	25 E-7 De-Riveting Review w/DOE/WHC/JPL - Valley Forge - *Hemler, et al*	26	27	34
SEPTEMBER	28	29	30	31	1	2	3	35
	4 HOLIDAY	5	6 Installation of the RTD Cable Assembly on F-5 - Mound - Miamisburg, OH - *Retnstrom/Gosling/Rickenbach/Douglas/Collingwood/Kiley*	7	8	9	10	36
	11	12	13 Titan Cassini Technical Advisory Committee Meeting - Denver, CO - Haley	14 Reentry Variability/ Uncertainty - Sandia National Labs - *Braun, Letts* F-5 Magnetics Segment Readiness Review - Mound - Miamisburg, OH - *Cockfield*	15	16	17	37
	18	19	20 Monthly Program Review - OSC Germantown, MD - Hemler, Braun, Retnstrom, Cockfield Fireball Effects - Sandia National Labs - Rosko	21 Reentry Variability/ Uncertainty Working Meeting w/DOE Analysis Team - Valley Forge - *Braun, et al*	22 Monthly Reports Due to DOE	23	24	38
	25	26 Mtg. with MET Chairperson - San Jose - Ha, Deane Databook Issues - LM-SLS, Denver, CO - Rosko	27	28 Reentry Variability/ Uncertainty Working Meeting w/INSRP - Valley Forge - *Braun, et al*	29	30	1	39

Cassini RTG Program Calendar

As of 18 October 1995

4th Qtr 1995

	M	T	W	T	F	S	S	FW
OCTOBER	2	3	4	5	6	7	8	40
		F-5 Thermal Vacuum Test - Mound Labs - Miamisburg, OH - *Haley/Kelly/Tobery*		Engineering Fragment Safety Test - Sandia Labs - *Hartman/Gosling*				
	9	10	11	12	13	14	15	41
	16	17	18	19	20	21	22	42
		Monthly Reports Due to DOE			Annual Reports Due to DOE			
	23	24	25	26	27	28	29	43
		RTG Assembly Walkthrough at Mound - Miamisburg, OH - *Reinstrom, Gosling*		Safety Analysis PSSP/RESP INSRP Review Meetings - Sheraton, Valley Forge - *Braun, et al*				
NOVEMBER	30	31	1	2	3	4	5	44
			Quarterly Program Review w/DOE - OSC, Germantown, MD *Hemler, Braun, Cockfield/Reinstrom*					
	6	7	8	9	10	11	12	45
		INSRP MET/BEES - Houston, TX - *Braun, Deane, Ha*						
	13	14	15	16	17	18	19	46
	20	21	22	23	24	25	26	47
			Monthly Reports Due to DOE	Holiday	Holiday			
DECEMBER	27	28	29	30	1	2	3	48
	4	5	6	7	8	9	10	49
	11	12	13	14	15	16	17	50
	18	19	20	21	22	23	24	51
					Monthly Reports Due to DOE			
	25	26	27	28	29	30	31	52
	Holiday							

Cassini RTG Program
Technical Report Distribution

BANNAN, K.M.	Space Power Library (2)
BRAUN, J.F	29B12 Bldg. B
BRANDT, D.	U4019 Bldg. 100
BUCKLEY, J.	U3040 Bldg. 100
BURGER, C.F.	20B41 Bldg. B
CENTURIONI, D.	Mezz Bldg. B
COCKFIELD, R. D.	20B41 Bldg. B
COLE, D.	M4018 Bldg. 100
CURRAN, J.	Mezz Bldg. B
DADD, S.	Mezz Bldg. B
DAYWITT, J.	U4019 Bldg. 100
DEANE, N.	San Jose Office
DE FILLIPO, L.E.	29B12 Bldg. B
DICKINSON, K.	29B12 Bldg. B
DOUGLAS, L.	Mezz Bldg. B
DOWER, A. G.	U7035 - Bldg. 100
FRANKLIN, B.	Mezz Bldg. B
GRIMLEY, B.	Mezz Bldg. B
HALEY, V.F.	29B12 Bldg. B
HARTMAN, R.F.	29B12 Bldg. B
HEMLER, R.J.	29B12 Bldg. B
KAIN, S.A.	29B12 Bldg. B
KAUFFMAN, R.	20B41 Bldg. B
KELLY, E.	20B41 Bldg. B
KLEE, P.M.	20B41 Bldg. B
KLINE, T.F.	29B12 Bldg. B
KUGLER, W.	20B41 Bldg. B
LETTS, B.	U7026 Bldg. 100
MONTGOMERY, J. L.	29B12 Bldg. B
MORGAN, E. M.	U3040 Bldg. 100
MORGAN, R. E.	29B12 Bldg. B
MURRAY, M.	29B12 Bldg. B
NAKAHARA, J.	29B12 Bldg. B
NYCE, R.	Mezz Bldg. B
REINSTROM, R.M.	29B12 Bldg. B
ROSKO, R.	20B41 Bldg. B
SAYDAH, A.R.	29B12 Bldg. B
SERENI, M.	Mezz Bldg. B
TOBERY, W.	20B41 Bldg. B
VICENTE, F.A.	29B12 Bldg. B
VIJAIYAN, K.	(FAX) DOE Canoga Park, CA
WAKS, J. M.	29B12 Bldg. B
ZULA, G.C.	29B12 Bldg. B

Inform Sally Kain X1597 of any changes, additions, or deletions.

sak 3:Dist 10/4/95